AD_____

Award Number: DAMD17-99-1-9555

TITLE: Evaluation of Early and Prolonged Effects of Acute Neurotoxicity and Neuroprotection Using Novel Functional Imaging Techniques

PRINCIPAL INVESTIGATOR: Anna-Liisa Brownell, Ph.D.

CONTRACTING ORGANIZATION: The Massachusetts General Hospital
Boston, Massachusetts 02114

REPORT DATE: August 2002

TYPE OF REPORT: Annual

PREPARED FOR: U.S. Army Medical Research and Materiel Command
Fort Detrick, Maryland 21702-5012

# REPORT DOCUMENTATION PAGE

Form Approved
OMB No. 074-0188



| 1. AGENCY USE ONLY (Leave blank) | 2. REPORT DATE | 3. REPORT TYPE AND DATES COVERED |
|---|---|---|
| | August 2002 | Annual (15 Jul 01 - 15 Jul 02) |

**4. TITLE AND SUBTITLE**
Evaluation of Early and Prolonged Effects of Acute Neurotoxicity and Neuroprotection Using Novel Functional Imaging Techniques

**5. FUNDING NUMBERS**
DAMD17-99-1-9555

**6. AUTHOR(S)**
Anna-Liisa Brownell, Ph.D.

**7. PERFORMING ORGANIZATION NAME(S) AND ADDRESS(ES)**
The Massachusetts General Hospital
Boston, Massachusetts 02114

Email: abrownell@partners.org

**8. PERFORMING ORGANIZATION REPORT NUMBER**

**9. SPONSORING / MONITORING AGENCY NAME(S) AND ADDRESS(ES)**
U.S. Army Medical Research and Materiel Command
Fort Detrick, Maryland 21702-5012

**10. SPONSORING / MONITORING AGENCY REPORT NUMBER**

**11. SUPPLEMENTARY NOTES**
report contains color

**12a. DISTRIBUTION / AVAILABILITY STATEMENT**
Approved for Public Release; Distribution Unlimited

**12b. DISTRIBUTION CODE**

**13. Abstract** *(Maximum 200 Words)* *(abstract should contain no proprietary or confidential information)*

We have proposed to explore the relationship between impairments in functional and metabolic pathways and regional neural dysfunction, and the efficacy of neuroprotection provided by a metabotropic glutamate receptor agonist. We have conducted studies using a super-high resolution positron tomograph to explore acute and long-term excitotoxicity mediated mechanisms in rats exposed to 3-nitroproprionic acid (3-NP). We have also conducted studies of glucose metabolism in transgenic mice expressing Huntington's gene. Complementary magnetic resonance spectroscopy studies to explore changes in neurochemicals were conducted in both 3-NP treated rats and transgenic mice as well. We tested also neuroprotection against 3-NP induced neurotoxicity with metabotropic glutamate receptor agonist; ABHxD-I. These studies showed that ABHxD-I could protect during the injection period, but after it, 3-NP induced striatal degeneration continues. Studies of dopamine receptors (D1 and D2) as well as dopamine transporters showed a gradually decreased binding following 3-NP administrations both in protected and non-protected 3-NP rats. In HD mice, a progressive age related degeneration of glucose metabolism was observed correlating with decrease in N-acetyl-aspartate detected with MRS. Dopamine receptor and transporter bindings were significantly reduced compared to littermate controls. Studies of glutamate receptors showed locally decreased binding in striatum and in cortex following 3-NP. In addition, technical goals of algorithm development for data acquisition, image reconstruction, and data analyses were met.

**14. SUBJECT TERMS**
neurotoxin, positron emission tomography, glucose metabolism, dopamine receptors, glutamate receptors, metabotropic glutamate

**15. NUMBER OF PAGES**
71

**16. PRICE CODE**

| 17. SECURITY CLASSIFICATION OF REPORT | 18. SECURITY CLASSIFICATION OF THIS PAGE | 19. SECURITY CLASSIFICATION OF ABSTRACT | 20. LIMITATION OF ABSTRACT |
|---|---|---|---|
| Unclassified | Unclassified | Unclassified | Unlimited |

## Table of Contents

# THIRD ANNUAL REPORT "Evaluation of Early and Prolonged Effects of Acute Neurotoxicity and Neuroprotection Using Novel Functional Imaging Techniques"

## INTRODUCTION

Exogenous and/or endogenous neurotoxicity has directly or indirectly related to various neurodegenerative diseases including Parkinson's and Huntington's disease (Reiter et al 1998, Gorrell et al 1996, Zayed et al 1996, Checkoway et al 1999, Mizuno et al 1999, Hattori et al 1998, Schapira et al 1996 ). Therefore it is a major challenge to develop specific and sensitive in vivo methods to investigate pathophysiological mechanisms of toxins. This information is essential in order to design new methods for neuroprotection and therapy. Our overall research goal is to develop and improve in vivo imaging techniques to examine neuro-function of glutamatergic and dopaminergic receptors as well as oxidative glucose metabolism and neurochemicals. We particularly focus our efforts in exploring the excitotoxicity induced regional neuronal dysfunction in functional and metabolic pathway. The neuronal toxicity models include 3-nitropropionic acid induced striatal lesions and transgenic mice with gene expression of human Huntington's disease (HD). In the final phase of this project we will test neuroprotection with novel newly developed metabotropic glutamate receptor agonist.



## BODY

The third grant year included longitudinal imaging studies of energy metabolism, dopamine and metabotropic glutamine receptor function in rodent Huntington disease (HD) models; 3-nitropropionic (3-NP) rats and HD transgenic mice. Neuroprotection with metabotropic glutamate receptor agonist was tested in 3-NP rat model. In addition, further development of super-high resolution PET imaging techniques was conducted to enable to produce highly repeatable imaging studies in longitudinal imaging sessions. This was done especially with the second generation super high resolution PET system, where sensitivity for radioisotope detection was about 4 times higher than the system, we have used earlier. This enabled significant improvement for imaging of mice (Figures 1-3, Appendix), which are highly limited for the volume of injected ligand so that only small amount of radioactivity can be introduced into a target tissue. Also significant development of radiolabeling and evaluation of metabotropic glutamate receptors was done. Progress in the different areas is evaluated in the following.

**1. Technical tasks:** Further development of imaging techniques was conducted during the third grant year. These tasks included further development of a computer driven imaging table for the second super-high resolution positron emission tomography (PET) device. To be mentioned that design and construction of this second generation super high resolution PET imaging device is supported by the Department of Defense grant to Dr. Jack Correia at the Massachusetts General Hospital.

During the third year, further effort was used for development of software for data acquisition, implementation of image reconstruction programs to the unix (linux) based computer system and development of image analyses for multimodality data co-registration (Canales and Brownell, "New approaches in parametric imaging – use of direct algorithm", Appendix). This data analyzing technique was also extended to primate studies (Manuscript; Brownell et al, "Mapping of brain function after MPTP induced neurotoxicity in a primate Parkinson's disease model", Appendix). The experimental primate studies has been a collaborative work with Dr. Ole Isacson at McLean Hospital, Belmont and it has been also funded by the Department of Defense to Dr. Isacson.

a) **Computer controlled imaging "table":** During the earlier grant years we developed a basic model of computer controlled imaging "table" for the small super-high resolution positron emission tomograph. During the third grant year we further optimized it. The "table", which includes a stereotactic headholder with earbars and mouth (teeth) bar is designed separately for rat and mouse, because the size of the head of these two species is significantly different, as well as the other experimental maneuvering, to prepare animals for imaging studies. In addition, we conducted detection of radioactivity over the heart in mice studies and the table has to move back and forth to sequentially detect activity in heart and brain areas (Figure 1, Appendix).

b) **Software development:** Software was developed to control the movement of the imaging "table" electronically to scan through selected body areas slice by slice. Image reconstruction programs have also been updated and further developed to run in modern high speed PC computers, both in MS Windows and unix (linux) based systems.

   The computer system controlling the PET device is a window PC system and PET data is obtained in an in-house developed PC data format. Magnetic resonance imaging and spectroscopy (MRS) are acquired using unix based systems. To be able to perform image comparison and data fusion of PET and MRI/MRS we have developed further programs to make PET data compatible to the systems (Canales and Brownell, "New approaches in parametric imaging – use of direct algorithm", Appendix).

   The other challenge in software development has been to develop high resolution imaging techniques for multimodality registration. The technique we are using now is based on volume rendering of MR images and fusion of MR and PET images based on the Normalized Mutual Information (NMI) algorithm (Manuscript; Brownell et al, "Mapping of brain function after MPTP induced neurotoxicity in a primate Parkinson's disease model", Appendix).

**2) Radiopharmaceutical development:** Dr. Alan Kozikowski has synthesized (Kozikowski et al 1998) and provided us the precursor for labeling of metabotropic glutamate receptor agonist; (methyl-2-(methoxycarbonyl)-2-(methylamino) bicycle[2.1.1] -hexane-5- carbocylate (MMMHC). We have successfully labeled the amine precursor

with C-11 methyl triflate and a yield of 120 mCi of the labeled product has been obtained (Figure 4, Appendix). This labeled ligand goes through the blood brain barrier (Figures 5 and 6) and we hypothesize that it will be metabolized to (2-aminobicyclo [2.1.1]hexane-2,5-dicarboxylic acid-I (ABHxD-I) in the brain tissue through esterase and aminase (Figure 4, Appendix). Dr. Kozikowski and his team have shown that ABHx-D-I binds both on group I and II metabotropic glutamate receptors. Reported EC50 values are mGluR2 (0.33uM) > mGluR5 (0.72 uM) > mGluR1 (1.6 uM) > mGluR3 (2.2 uM) > mGluR6 (5.3) > mGluR4 (23 uM) (Kozikowski et al1998, Conti et al 2000). We are now testing with his team, if the radiolabeled product we use in the imaging studies, has the same receptor binding profile as ABHxD-I. This missing confirmed information has delayed finalizing of Dr. Meixiang Yu's manuscript of "C-11 labeling and in vivo evaluation of [11C] (1S2S4S5S) dimethyl 2-(methylamino) bicyclo[2.1.1]hexane-2,6-dicarboxylate".

**3) Biological experiments:**

**a) Experiments and animals:** During the third year, neuroprotection was tested with metabotropic glutamate receptor agonist; ABHxD-I, in ten 3-NP rats using 2 different treatment paradigms; single dose and multiple dose administrations. Longitudinal imaging studies were conducted in the protected and 5 non-protected (3-NP administration only) rats (male Spraque-Dawley) and 16 HD transgenic and 6 littermate control mice. Altogether 65 PET imaging sessions and 9 MRI-MRS imaging sessions were conducted. Imaging characteristics of the radiolabeled ligand (11C-MMMHC) were tested also in additional 6 control rats, one control primate and one MPTP-treated primate. In addition, microdialysis was conducted in 2 rats to evaluate a profile of neuroprotective ligand (ABHxD-I) in the striatum.

**b) Experimental procedures in rats:** Because neuroprotection was a significant part of the third year's research effort; we tested first accumulation pattern and time course of 11C-MMMHC in 2 rats using ip. and iv. administration of the ligand. Because the accumulation in the brain after iv. injection was significantly faster and higher than with ip. injection, we decided to use iv. injection for both administration of neurotoxin (3-NP) and neuroprotective ligand (ABHxD-I). In addition, inter animal variation in the response of 3-NP after iv. injection is supposed to be smaller than with multiple injections (Guyot et al 1997).

Nine rats were administered with iv. administration of 3-NP (10 mg/kg iv., 2 times a day for 5 days or until symptomatic (gait observed). Six of these rats were injected with neuroprotective ligand (ABHxD-I) 2 times a day; 30 min before 3-NP injection, with a dose 5 mg/kg/day. Six rats were injected with a single high dose of 3-NP (30 mg/kg iv.) Four of these rats had a single injection of neuroprotective ligand (ABHxD-I, 5 mg/kg iv.) 30 min before 3-NP.

During the 3-NP treatment period, rats were individually housed in the metabolic cages, and their diet and excretion was closely followed. For imaging studies rats were anesthetized with halothane (1-1.5% with oxygen flow rate of 3 L/min). Catheters were introduced into the tail vein for administration of protective ligand, 3-NP and

radiolabeled ligands and into the tail artery for collection of blood samples to determine glucose level and blood input function needed for quantification of glucose metabolic rate and/or receptor binding.

Microdialysis was conducted in 2 rats to evaluate metabolic profile of neuroprotective ligand (ABHxD-I). Concentric dialysis probes (membrane: 18 KDa cutoff, 200 mm o.d., length 4 mm) were implanted into the right striatum 18-24 h before the perfusion. Rats were anaesthetized with halothane and placed in a stereotaxic frame with an incisor bar set at -3.3 mm below an interaural line. After the skull was exposed and a burr hole drilled, the probe was slowly (2-3 min) lowered into the targeted region and secured to the skull bones. The coordinates of the probe's tip were: AP+0.5; ML 2.7; V -7.2 for striatum. : AP -3.8; ML 0.8; V 5.8 for thalamus, and: AP 2.2; ML 4.5; V-3.5 for frontal cortex. The perfusion medium (145 mM NaCl, 2.7 mM KCl, 1.2 $CaCl_2$, 1.0 mM $MgCl_2$, pH 7.4) was delivered at 1 ml/min using a microperfusion pump (CMA/100, CMA, Acton, MA) and dialysate samples were collected every 10 min into 5 ml of 0.5M perchloric acid. Collection of basal dialysate samples started after 1 hour of perfusion. After completion of the experiments the rats were sacrificed and location of the probes in the striatum verified. ABHxD-I content and time course will be analyzed of dialysates using mass spectrometer. However, the final analyzed data is not yet available.

**c) Results in rats:**

***Behavior:*** Even using iv. administration of neurotoxicity, there is a significant interanimal variation in response of 3-NP toxication on locomotor activity. In analyzing motor score we used a method, based on the motor deficit score by Quary et al 2000 (Guyot et al 1997, Quary et al 2000). Briefly, intermittent dystonia of one hindlimb, score=1; intermittent dystonia of two hind limbs, score=2; permanent dystonia of hind limbs, score=3; gait abnormalities consisting mainly of an uncoordinated and wobbing gait, score=4; recumbence lying on one side but showing uncoordinated movements when stimulated, score=5; near death by almost complete paralysis, score =6; in addition capability to grasp with their forepaws (able=0, unable=1) and capability to stay on small platform for 10 seconds (able=0, unable=1). Using these criteria six of the 15 rats showed significant hypokinesia, four of them died in a week having score >6 and two of them had hind limb paralyses and the motor score between 4 and 6. From the other nine rats, 4 showed some hypokinesia and gait and scored 2-3 and 5 showed light slowness and occasional uncoordinated gait and scored 0-1.

Table 1. Distribution of locomotor activity in the neuroprotected (ABHxD-I and 3 NP) and non-neuroprotected (3 NP only) groups within 2 different administration paradigms (multiple doses or single dose).

| | ABHxD-I and 3-NP | 3-NP only | Score > 6 | Score 4-6 | Score 2-3 | Score 0-1 |
|---|---|---|---|---|---|---|
| Multiple dose administration | 6(A) | 3(B) | | | | |
| | | | ABCD | AB | ABCD | AAACC |
| Single dose administration | 4(C) | 2(D) | | | | |

Quary et al (Quary et al 2000) found the similar inter animal variation in neurotoxic effects of 3-NP in Spraque Dawley rats and he proposed that the variation may be caused by genetic effects and is strain dependent. He was proposing to use of Lewis rats for experiments of neuroprotection since inter animal variation was significantly smaller in that strain compared to Spaque-Dawley rats.

***Imaging studies of glucose metabolism:*** PET imaging studies of glucose metabolism were conducted using $^{18}$F-2-fluorodeoxy-D-glucose as tracer in all 3-NP treated rats. Nine 3-NP treated rats were imaged before and during 3-NP administrations, and 2 days and 1 week post 3-NP. Six of these rats had administration of neuroprotective agent; ABHxD-I, 30 min before administration of 3-NP.

Daily PET imaging studies during 3-NP administration showed that there was no difference in protected and non-protected groups in cortex or striatum after one day of starting 3-NP injections. The average decrease of glucose utilization was between 4 and 8%.

On the third 3-NP injection day, the protected group had even enhanced values for glucose utilization in striatum. Inter animal variation was, however, significant. The change of glucose utilization compared to pre 3-NP values in the striatal area was between -8 and +9% in the protected group, while in the non-protected group it was between -6 and -20%. At that time point, there was no difference between groups concerning cortical degeneration.

One day after cessation of 3-NP injections, glucose utilization had recovered in the protected group in the cortical area being 0 to +5% over pre 3-NP values, while the changes in the striatal values were between -6 and +4% from the pre 3-NP values. There was no recovery in the non-protected group. However, 1 week later progressive degeneration continued in both groups. In the protected group, the cortical values were decreased by -4 and -21% and striatal values -9 and -13 % from the pre 3-NP values. The decrease in non-protected group was even higher being -30 to -35 % in cortical area and -35 to -40% in striatum.

Acute neuroprotection was tested in 4 rats using a single high dose administration of 3-NP proceeding with a single dose of ABHxD-I. Decrease of glucose utilization 2 days later was between -30 and -35% in cortex and between -20 and -29% in striatum in the protected group and between -40% and -45% both in cortex and striatum in the non-protected group.

***Imaging studies of dopamine receptors:*** We conducted imaging studies of dopamine D1 and D2 receptors and dopamine transporters in all rats before 3-NP injections and 2 days and 1 week post 3-NP. Dopamine D1 receptors were imaged with $^{11}$C-SCH (Schoering 23390) and dopamine D2 receptors with $^{11}$C-raclopride. Dopamine transporters were imaged with $^{11}$C-CFT (2β-carbomethoxy-3β-(4-fluorophenyl tropane). We obtained unexpected results of dopamine receptor function in protected and non-protected groups. Actually in all protected animals dopamine receptor binding (D1, D2 receptors and dopamine transporter) was lower than that in non-protected animals (Figures 7a and b, Appendix). Dopamine D2 receptor binding was 42-51% lower in protected group than in

non-protected group. Correspondingly, dopamine transporter binding was 13-32% lower in the protected group.

***Imaging studies of metabotropic glutamate receptors:*** Imaging studies of metabotropic glutamate receptors are the most exiting imaging approach, what has happened for a while. These imaging studies will open a new window for large variety of neurodegenerative diseases exploring defects in functions localized in striatal or cortical areas. We have done significant progress with the labeling aspects as well as experimental imaging aspects. However, we do not know yet, if the labeled product; 11C-MMMHC, has the same receptor-binding scheme as the end point product ABHxD-I has. These binding studies are progressing with collaboration with Dr. Kozikowski, who developed the original ligand. Based on the imaging studies, we know that the labeled ligand goes fast into the brain and in 2-3 min equilibrium time will be irreversibly bound in cortical and striatal areas, average binding level being 6-8%. This binding pattern was locally decreased in cortex and striatum after 3-NP toxicity; -20 – -30% in cortex and -25 – -35% in striatum 2 days after 3-NP (Figure 7a, Appendix).

Since ABHxD-I has affinity also to subgroup I metabotropic glutamate receptors, EC50 values being for mGluR5 0.72 μM and mGluR1 1.6 μM, we investigated 11C-MMMHC (radiolabeled ester product) distribution in a primate brain (Macaca fascicularis) before and after MPTP neurotoxicity. In these primate studies we observed similar decrease in glutamate receptor binding, we did in 3-NP rat model. 11C-MMMHC binding was decreased in caudate -36 +/- 6%, in putamen -38 +/- 7% and in primary motor cortex -46 +/- 10%. We determined also dopamine transporter binding with 11C-CFT after MPTP, because it is the most affected dopamine function in MPTP toxication. The decrease in caudate was -50 +/- 12% and in putamen -52 +/- 12%. Blood flow in these sites was also decreased; -12 +/-5% in caudate, -16 +/-7% in putamen and -28 +/-13% in primary motor cortex Figures 5 and 6, Appendix).

***Imaging studies of anatomy and neurochemicals (MRI/MRS studies):*** Imaging studies of neuroanatomy have been used to identify location and size of lesions and to record brain anatomy for volumetric image rendering. In earlier studies, MRS studies of neurochemicals have shown elevated peaks of lactate and macromolecules as well as succinate immediately after 3-NP toxicity. Using this information, we developed a single dose administration technique for 3-NP to record lesion development in real time, as formation of succinate peak.

We observed that in protected group succinate peak was developed but no lactate was observable in 3 hours follow up time. In non-protected group both succinate and lactate peaks were formed during this follow up time. Similar observations of acute temporal changes in succinate formation after 3-NP toxication has been published by Lee (Lee et al 2000).

***Histological confirmation of neural loss:*** Histological endpoint studies were conducted in 6 rats to confirm the neural loss after 3-NP and possible protection factor in the rats treated with neuroprotective ligand; ABHxD-I.

Dr. Francesca Cicchetti has done these histological analyses. She has done both calbindin immunoreactivity and immunochemical determination of metabotropic

glutamate2/3 receptors (Figures 8 and 9, Appendix). These histological studies support the observation done with studies of glucose utilization.

Dr. Alp Dedeoglu, who used to work with Dr. Flint Beal, when he was at Massachusetts General Hospital, did the earlier analyses and Nissl staining.

***Evaluation of neuroprotection:*** We investigated characteristics of metabotropic glutamate receptor agonist; ABHxD-I as a neuroprotective agent. These experiments show that we were able to show a trend for neuroprotection as less decrease in glucose utilization and glutamate receptor binding after 3-NP neurotoxicity than in non-protected animals. However, dopamine receptor binding decreased in all protected animals more than in non-protected animals.

Since glucose utilization is a major energy source of the brain, the change in glucose utilization can be a sensitive indicator for the energy dysfunction in the brain. 3-NP, a permanent inhibitor of succinate dehydrogenese (Johnson et al 2000) can disrupt the mitochondrial function, decrease glucose utilization and cause striatal degeneration (Storgaard et al 2000, Guyot et al 1997, Bowyer et al 1996). Interestingly, Reynolds et al (Reynolds et al 1998) published that dopamine deficiency may protect against 3-NP toxicity and Johnson et al (Johnson et al 2000) published that long term exposure to 3-NP increases dopamine turnover.

In our experiments, neuroprotection with ABHxD-I originates dopamine receptor deficiency and enhance glucose utilization. However, we have not yet been able to resolve mechanism and time course of these changes and these tasks are under investigation. We conducted microdialyses studies to record time course of appearance ABHxD-I in the rat striatum. The mass spectrometric analyses of the drug in the CNS samples are underway.

**d) Imaging studies in mice:** We conducted longitudinal imaging studies of glucose metabolism, dopamine D1 and D2 receptors and dopamine transporters in Huntington's disease mouse model and littermate controls. Technical arrangement of experimental imaging procedures with a super-high resolution PET system is presented in Figure 1 (Appendix). The slice thickness is 1.5 mm and studies were performed with 1.25 mm steps. Longitudinal analyses of glucose utilization in HD mice showed in striatum a progressive decrease of 0.05%/day (Figure 2, Appendix). However, in some HD mice an early enhancement of striatal glucose utilization was observed. Dopamine transporter binding was 40 - 55% lower in HD mice compared to littermate controls. No age related decline was observed in transporter binding. 11C-raclopride binding in dopamine D2 receptors was decreased by -40 - -50% at the age of 8 weeks and further decreased being 60 - 65 % lower that littermate controls at the age of 12 weeks. 11C-SCH (Shoering compound 23 390) binding in dopamine D1 receptors was decreased by -10 - -20 % at the age of 8 weeks and further decreased being 45 - 55% lower than in littermate controls at the age of 12 weeks (Figure 3, Appendix).

## KEY RESEARCH ACCOMPLISHMENT

- further enhancement of imaging "tables" with stereotactic headholders especially for mouse studies

- further development of software for data acquisition and reconstruction for modern PC and linux based systems and the second super high resolution PET device

- further development and testing of image algorithms for image reconstruction for multi modality image co-registration

- observation of significant inter animal variation in the response to 3-NP induced neurotoxicity both in high dose single or low dose multiple injection procedures in motor activity and energy metabolism

- observation that development of striatal lesion after administration of 3-NP can be registered in real time using MRS and detection of succinate formation

- observation that striatal lesions with energy deficit show progressive decrease in dopamine D1 and D2 receptor

- observation that dopamine transporter binding is slightly increased immediately after 3-NP treatment and progressively decreases later

- observation that after 3-NP treatment, metabotropic glutamate receptor binding is decreased focally in striatal and cortical area, which also show decreased glucose utilization

- observation that after MPTP treatment the same metabotropic glutamate receptor ligand had also affinity to mGluR1 and mGluR5 receptors and had locally decreased binding in striatal and cortical area which also showed decreased blood flow and significantly decreased striatal dopamine transporter binding

  observation that MRS shows increased succinate immediately after 3-NP and can be used in real time to follow development of lesion and effect of neuroprotection

  observation that ABHxD-I develops neuroprotection against 3-NP toxicity by enhancing glucose utilization and dopamine receptor degeneration

  observation that ABHxD-I protection accelerates washout of 11C-CFT, 11C-raclopride and 11C-SCH and decrease corresponding receptor binding

- observation that decreasing of glucose utilization as well as NAA is linearly correlated with age in the striatum of HD mice

## REPORTABLE OUTCOME

Anna-Liisa Brownell, Y. Iris Chen, Kelly Canales, Robert Powers, Ole Andreasson, Flint Beal, Bruce Jenkins. Glucose utilization assessed by high resolution PET with comparison to MRI/MRS in a transgenic mouse model of Huntington's disease. HiRes2001, Meeting on High Resolution Imaging in Small Animals: Instrumentation, Applications and Animal Handling, September 9-11, 2001, Rockville, Maryland.

A-L Brownell, YI Chen, KE Canales, RT Powers, A Dedeoglu, FM Beal, BG Jenkins. 3-NP induced neurotoxicity – assessed by ultra high resolution PET with comparison to MRI and MRS. 31st Annual Meeting of Neuroscience. San Diego, November 10-15, 2001

A-L Brownell, YI Chen, KE Canales, E. Livni, RT Powers, A Dedeoglu, FM Beal, BG Jenkins. 3-NP induced neurotoxicity – assessed by ultra high resolution PET with comparison to MRI and MRS. 1st Annual Meeting of the Society for Molecular Imaging. Boston, August 24-26, 2002

K. Canales, A-L. Brownell. New approaches in parametric imaging -use of direct algorithm. 49th Annual Meeting of the Society of Nuclear Medicine. Los Angeles, June 15-19, 2002. The Journal of Nuclear Medicine 2002; 45:(S5):209.

A-L. Brownell, Y.I. Chen, K. Canales, B. Powers, B.G. Jenkins. Neural degeneration in a transgenic HD mouse model - an ultra high resolution PET study with comparison to MRI/MRS. 49th Annual Meeting of the Society of Nuclear Medicine. Los Angeles, June 15-19, 2002. The Journal of Nuclear Medicine 2002;45:(S5):61.

A-L. Brownell, K. Canales, Y.I. Chen, C. Owen, R. Powers, A. Kozikowski, D. Elmaleh, M. Yu. Metabotropic glutamate receptors - new targets for neuroimaging. 49th Annual Meeting of the Society of Nuclear Medicine. Los Angeles, June 15-19, 2002. The Journal of Nuclear Medicine 2002;45:(S5):110.

M.Yu, E. Livni, K. Nagren, K. Canales, R.Powers, D. Elmaleh, A. Kozikowski, A-L. Brownell. 11C-labeling of methyl 2-(methoxycarbonyl)-2-(methylamino) bicycle (2.1.1)hexane-5-carboxylate, a potent neuroprotective drug. 49th Annual Meeting of the Society of Nuclear Medicine. Los Angeles, June 15-19, 2002. The Journal of Nuclear Medicine 2002;45:(S5):167.

Anna-Liisa Brownell, Kelly Canales, Y.Iris Chen, Bruce G. Jenkins, Christopher Owen, Elijahu Livni, Meixiang Yu, Francesca Cicchetti, Rosario Sanchez-Pernaute, Ole Isacson. Mapping of brain function after MPTP induced neurotoxicity in a primate Parkinson's disease model. Brain 2002 (submitted)

Anna-Liisa Brownell, Iris Y. Chen, Xukui Wang, Meixiang Yu, Bruce G. Jenkins. Neurotoxicity (3-NP) induced changes in striatal dopamine receptor function. Parkinson's disease: The Life Cycle of the Dopamine Neuron. September 18-20, 2002 (submitted)

## CONCLUSIONS

The third grant year has been very successful and significant amount of biological information has been obtained regarding the 3-NP induced degenerative processes in energy metabolism as well as dopaminergic regulation during degeneration and after neuroptotection induced by metabotropic glutamate receptor agonist; ABHxD-I. We observed enhanced glucose utilization after 3-NP toxication in neuroprotected group while dopamine receptor binding was decreased compared to non-protected group. The mechanism of this process is under further investigation. Reynolds et al (Reynolds et al 1998) have published of a link between dopamine deficiency and striatal lesion formation after 3-NP toxicity. According to his experiments 6-hydroxydopamine induced dopamine deficiency protected against 3-NP toxicity in striatum. We observed using multiple administration protocol for 3-NP and ABHxD-I that ABHxD-I had a protective effect in striatum during the treatment period, but abolished after it; and 3-NP induced degeneration continued. Metabotropic glutamate receptors provide a new interesting insight to investigate the degenerative processes and their neuroprotective characteristics.

In the mouse model of HD, we observed significant age related decrease in dopamine D1 and D2 receptor binding. Dopamine transporter had also significant decrease but did not change with age.

During the third year, a number of technical tasks have also been accomplished including further development of computer controlled imaging "table" and other accessories needed to accomplish the whole project. Algorithm development for data acquisition, image reconstruction and data analyses have been very successful and automated programs are now running both in windows and linux based systems.

## REFERENCES


Borlongan CV, Koutouzis TK, Freeman TB, Hauser RA, Cahill DW, Sanberg PR. Hyperactivity and hypoactivity in a rat model of Huntington's disease: the systemic 3-nitropropionic acid model. Brain Res Brain Res Protoc 1997;1(3):253-7.

Bowyer JF, Clausing P, Schmued L, Davies DL, Binienda Z, Newport GD, Scallet AC, Slikker W Jr. Parenterally administered 3-nitropropionic acid and amphetamine can combine to produce damage to terminals and cell bodies in the striatum. Brain Res 1996; 712(2):221-9.

Checkoway H, Nelson LM. Epidemiologic approaches to the study of Parkinson's disease etiology. Epidemiology 1999;10(3): 327-36.

Conti P, Kozikowski AP. New synthesis of 2-aminobicyclo[2.1.1]hexane-2,5-dicarboxylic acid-I (ABHxD-I), a potent metabotropic receptor agonist. Tetrahedron Letters 0 (2000) 1-4.

Eradiri OL, Starr MS. Striatal dopamine depletion and behavioural sensitization induced by methamphetamine and 3-nitropropionic acid. Eur J Pharmacol 1999; 386(2-3):217-26.

Gorrell JM, DiMonte D, Graham D. The role of the environment in Parkinson's disease. Environmental Health Perspective1996; 104: 652-4.

Guyot MC, Hantraye P, Dolan R, Palfi S, Maziere M, Brouillet E. Quantifiable bradykinesia, gait abnormalities and Huntington's disease-like striatal lesions in rats chronically treated with 3-nitropropionic acid. Neuroscience 1997; 79(1):45-56.

Johnson JR, Robinson BL, Ali SF, Binienda Z. Dopamine toxicity following long term exposure to low doses of 3-nitropropionic acid (3-NPA) in rats. Toxicol Lett 2000; 116(1-2):113-8.

Kozikowski AP, Steensma D, Araldi GL, Tuckmantel W, Wang S, Pshenichkin S, Surina E, Wroblewski JT. Synthesis and biology of the conformationally restricted ACPD analogue, 2-aminobicyclo[2.1.1]hexane-2,5-dicarboxylic acid-I, a potent mGluR agonist. J Med Chem 1998; 41,1641-1650.

Lee W-T, Lee C-S, Pan Y-L, Chang C. Temporal changes of cerebral metabolites and striatal lesions in acute 3-nitropropionic acid intoxication in the rat. Magnetic Resonance in Medicine 2000; 44: 29-34.

Mizuno Y, Hattori N, Matsumine H. Neurochemical and neurodegenerative correlates of Parkinson's disease. Journal of Neurochemistry 1998;71(3): 893-

Quary S, Bizat N, Altairac S, Menetrat H, Mittoux V, Conde F, Hantraye P, Brouillet E. (2000). Major strain differences in response to chronic systemic administration of the

mitochondrial toxin 3-nitropropionic acid in rats: implications for neuroprotection studies. Neuroscience 2000; 97: 521-530

Reiter LM, DeRosa C, Kavlock RJ, Lucier G, Mac MJ, Melillo J, Melnick RL, Sinks T, Walton BT, The U.S. Federal framework for research on endocrine disruptors and an analysis of research programs supported during fiscal year 1996. Environmental Health Prespect 1998; 106: 105-113.

Reynolds DS, Carter RJ, Mortion AJ. Dopamine modulates the susceptibility of striatal neurons to 3-nitropropionic acid in the rat model of Huntington's disease. J Neurosci 1998; 18(23)1011-27.

Schapira A H V. Neurotoxicity and the mechanisms of cell death in Parkinson's disease. Advances in Neurology. L. Battistin, G. Scarlato, T. Carceni and S. Ruggieri. Philadelphia, Lippincott-Raven. 1996;69: 161-165.

Storgaard J, Kornblit BT, Zimmer J, Bert J, Gramsbergen P. 3-Nitropropionic acid in organotypic striatal and corticostriatal slice cultures is dependent on glucose and glutamate. Exp Neurol 2000; 164(1):227-35.

Zayed J, Mikhail M, Loranger S, Kennedy G, L'Esperance G. Exposure of taxi drivers and office workers to total and respirable manganese in an urban environment. American Industrial Hygiene Association Journal 1996; 57: 376-80.

## APPENDICES

**Figures 1-9.**

**Abstracts and reports:**

Anna-Liisa Brownell, Y. Iris Chen, Kelly Canales, Robert Powers, Ole Andreasson, Flint Beal, Bruce Jenkins. Glucose utilization assessed by high resolution PET with comparison to MRI/MRS in a transgenic mouse model of Huntington's disease. HiRes2001, Meeting on High Resolution Imaging in Small Animals: Instrumentation, Applications and Animal Handling, September 9-11,2001, Rockville, Maryland.

A-L Brownell, YI Chen, KE Canales, RT Powers, A Dedeoglu, FM Beal, BG Jenkins. 3-NP induced neurotoxicity – assessed by ultra high resolution PET with comparison to MRI and MRS. 31st Annual Meeting of Neuroscience. San Diego, November 10-15, 2001

A-L Brownell, YI Chen, KE Canales, E. Livni, RT Powers, A Dedeoglu, FM Beal, BG Jenkins. 3-NP induced neurotoxicity – assessed by ultra high resolution PET with comparison to MRI and MRS. 1st Annual Meeting of the Society for Molecular Imaging. Boston, August 24-26, 2002

K. Canales, A-L. Brownell. New approaches in parametric imaging - use of direct algorithm. 49th Annual Meeting of the Society of Nuclear Medicine. Los Angeles, June 15-19, 2002. The Journal of Nuclear Medicine 2002; 45:(S5):209.

A-L. Brownell, Y.I. Chen, K. Canales, B. Powers, B.G. Jenkins. Neural degeneration in a transgenic HD mouse model - an ultra high resolution PET study with comparison to MRI/MRS. 49th Annual Meeting of the Society of Nuclear Medicine. Los Angeles, June 15-19, 2002. The Journal of Nuclear Medicine 2002;45:(S5):61.

A-L. Brownell, K. Canales, Y.I. Chen, C. Owen, R. Powers, A. Kozikowski, D. Elmaleh, M. Yu. Metabotropic glutamate receptors - new targets for neuroimaging. 49th Annual Meeting of the Society of Nuclear Medicine. Los Angeles, June 15-19, 2002. The Journal of Nuclear Medicine 2002;45:(S5):110.

M.Yu, E. Livni, K. Nagren, K. Canales, R.Powers, D. Elmaleh, A. Kozikowski, A-L. Brownell. 11C-labeling of methyl 2-(methoxycarbonyl)-2-(methylamino) bicycle (2.1.1)hexane-5-carboxylate, a potent neuroprotective drug. 49th Annual Meeting of the Society of Nuclear Medicine. Los Angeles, June 15-19, 2002. The Journal of Nuclear Medicine 2002;45:(S5):167.

Anna-Liisa Brownell, Kelly Canales, Y.Iris Chen, Bruce G. Jenkins, Christopher Owen, Elijahu Livni, Meixiang Yu, Francesca Cicchetti, Rosario Sanchez-Pernaute, Ole Isacson. Mapping of brain function after MPTP induced neurotoxicity in a primate Parkinson's disease model. Brain 2002 (submitted)

Anna-Liisa Brownell, Iris Y. Chen, Xukui Wang, Meixiang Yu, Bruce G. Jenkins. Neurotoxicity (3-NP) induced changes in striatal dopamine receptor function. Parkinson's disease: The Life Cycle of the Dopamine Neuron. September 18-20, 2002 (submitted)

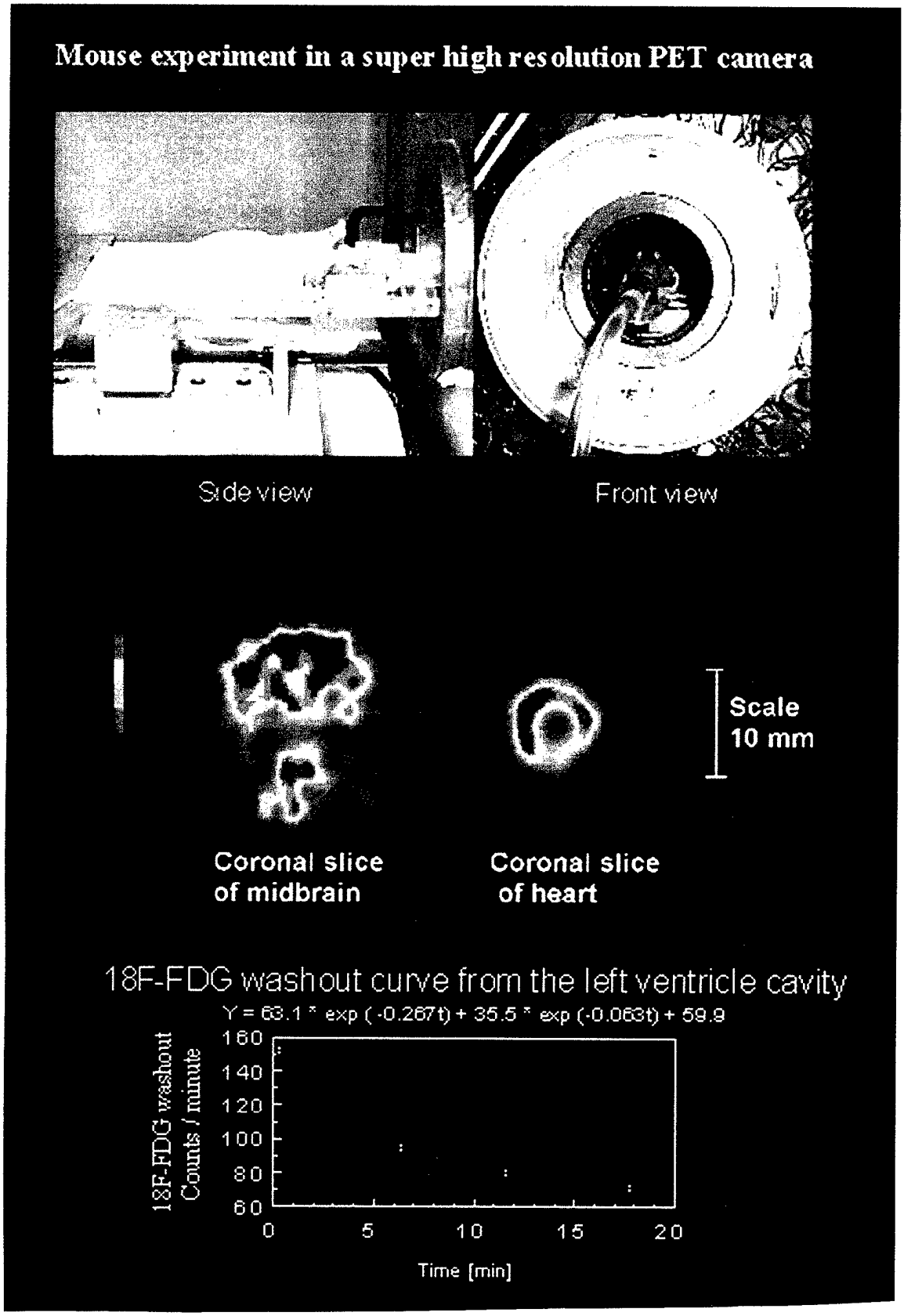


Figure 1. (top) Mouse experiment in a super high resolution PET camera.
(middle) Coronal slices of midbrain and heart to illustrate regional glucose utilization.
(below) Washout curve of radioactivity from the left ventricle detected by in vivo imaging over the heart.

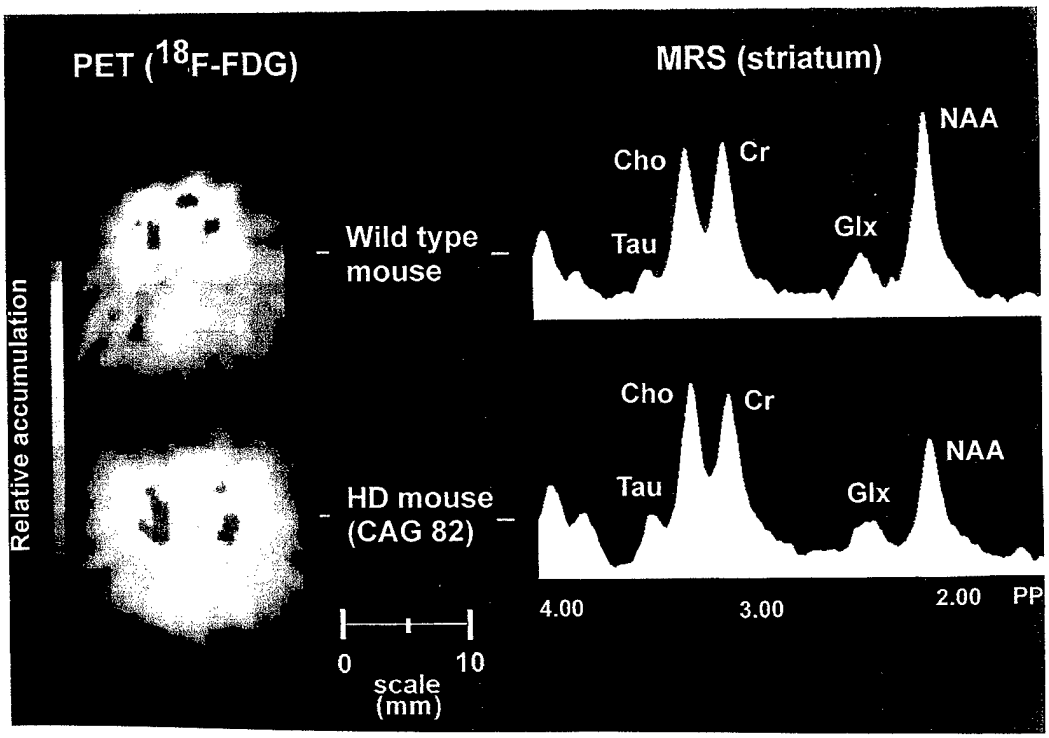


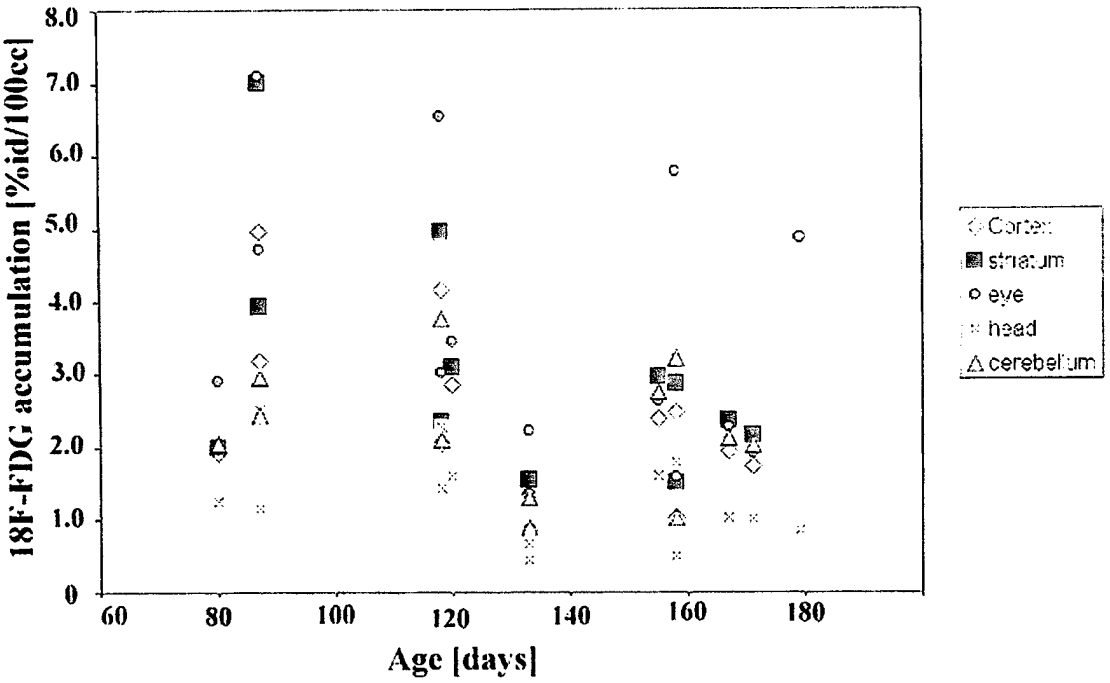


Figure 2. (above) Glucose utilization in a control and HD mouse and corresponding MRS studies of neurochemicals. (below) Percent distribution of 18F-FDG in cortex, striatum, eye, cerebellum and whole head during aging of the HD mice.

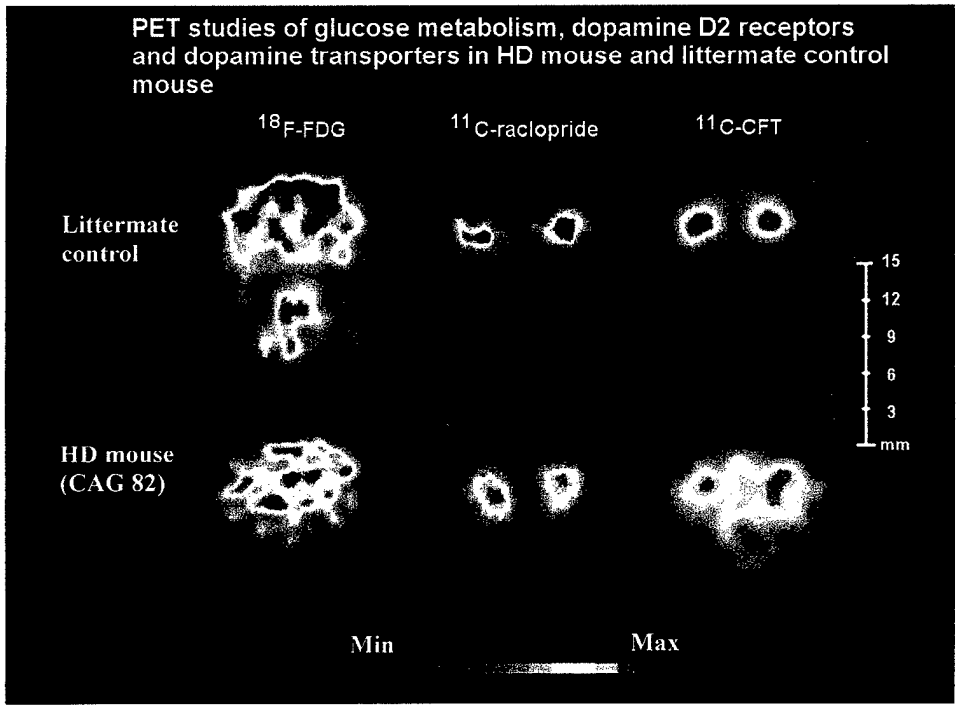


Figure 3. PET studies of glucose utilization, dopamine D2 receptors and dopamine transporters in HD mouse and littermate control.

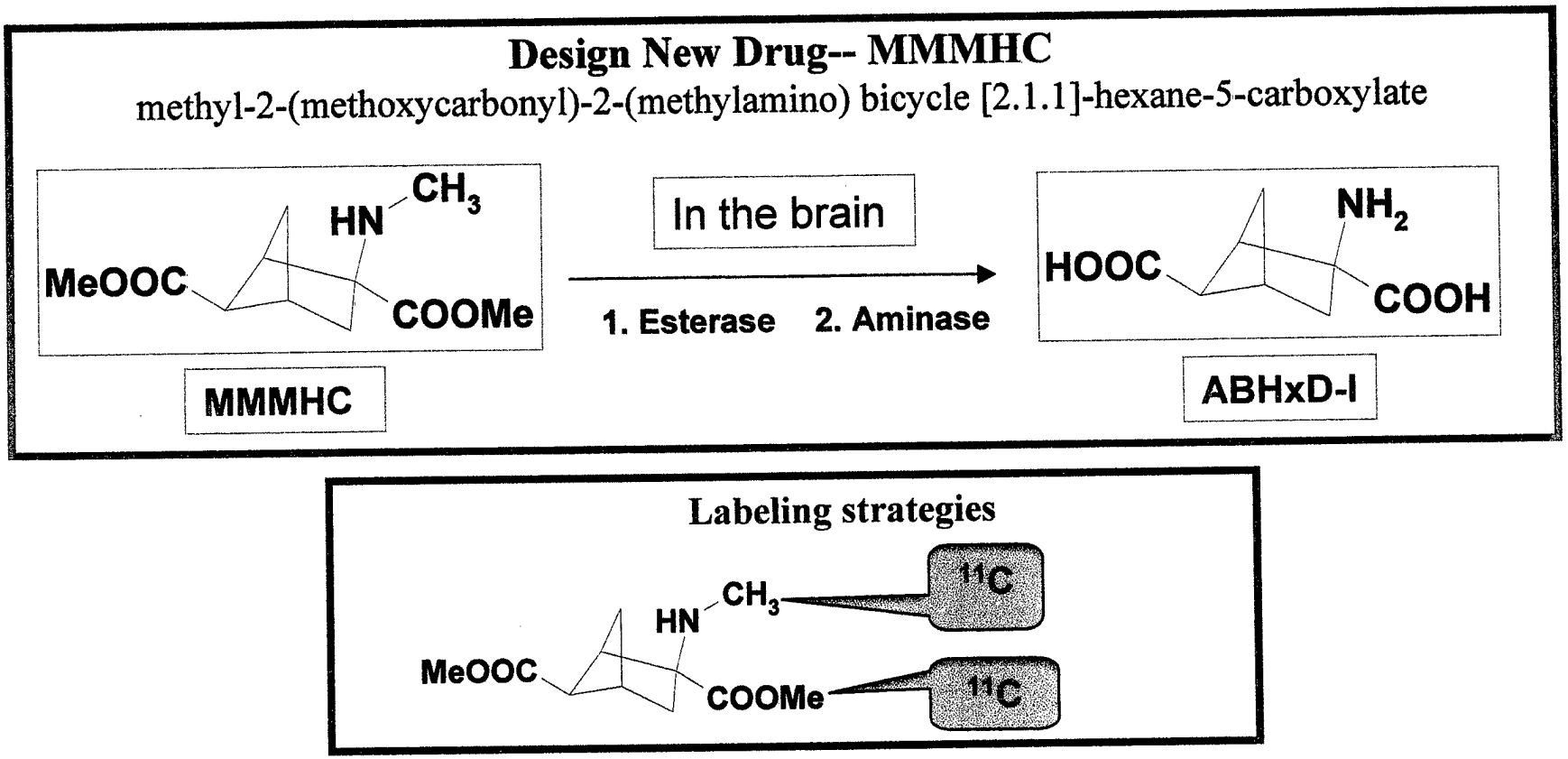


Figure 4. Schematic diagram of the radiolabeling of precursor for ABHxD-I with methyl iodide technique and carbon-11. (top) Expected metabolic pathway of the precursor ligand in the brain. (middle) Possible labeling sites for carbon-11. We used HN-CH3 link. (bottom) Radiochemical procedure to introduce carbon-11 to the precursor molecule.

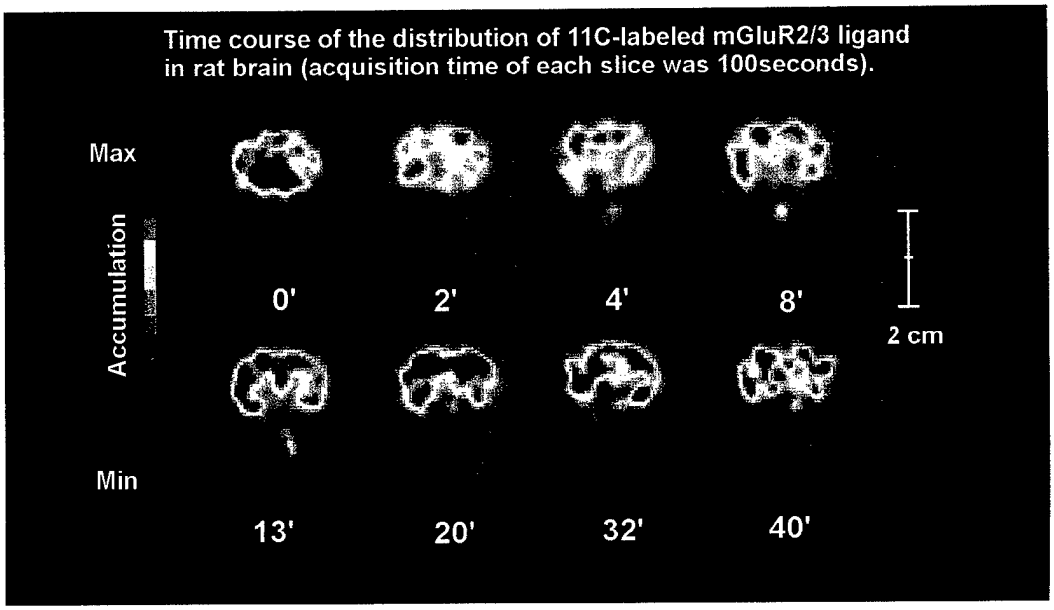


Figure 5. Time course of the distribution of 11C-MMMHC (mGluR2/3 receptor agonist) in a rat brain. Acquisition time of each slice was 100 seconds. The thickness of the midbrain slice is 1.3 mm. These images show that accumulation of 11C-MMMHC in cortical areas reach maximum level about 20 after injection of radioactivity.

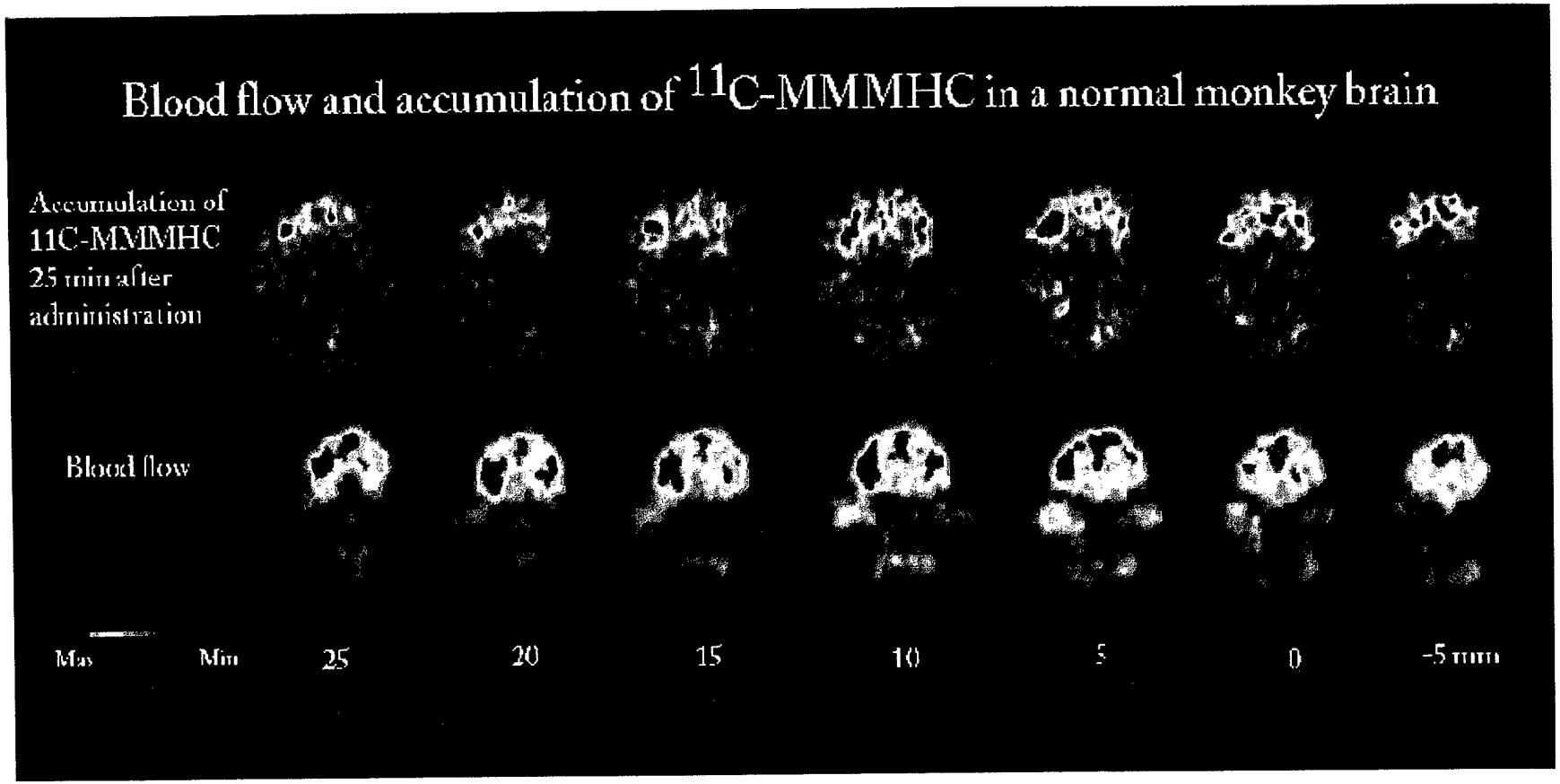


Figure 6. (top) Distribution of C-11 labeled mGluR receptor ligand (11C-MMMHC) 25 min after administration in the normal monkey (Macaca fascicularis) brain. (bottom) Blood flow study in the same animal. These images show that 11C-MMMHC binds dominantly in cortical areas.

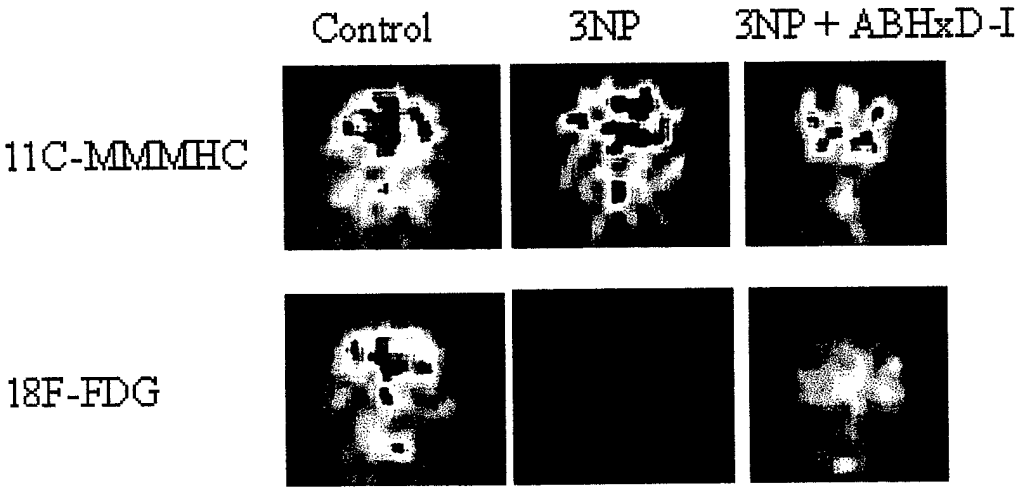


Figure 7a. Study of glucose utilization and binding of 11C-MMMHC in a control rat, a rat treated with 3-NP only (a high single dose) and a rat having neuroprotection with ABHxD-I 30 min before 3-NP injection (a high single dose). Imaging studies were done 2 days after 3-NP administration. These images clearly show enhanced glucose utilization in a rat protected with ABHxD-I compared to 3-NP only injected rat.

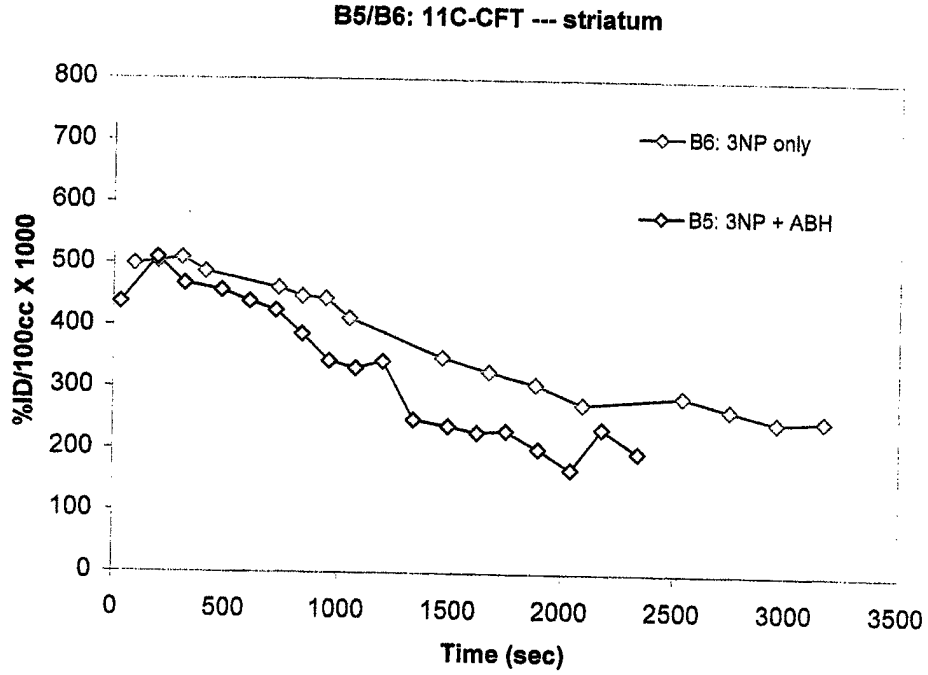


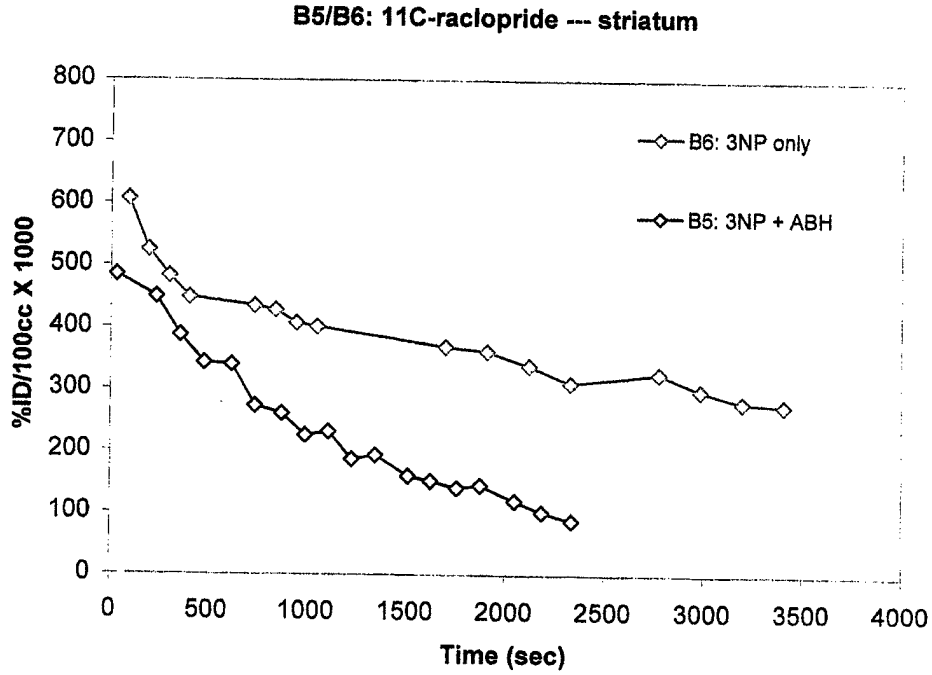


Figure 7b. Binding curves of 11C-CFT (binding in dopamine transporters) and 11C-raclopride (binding in dopamine D2 receptors) in the striatum of two rats; the other had 3-NP treatment only (B6) and the other had protection with ABHxD-I with 3-NP. ABHxD-I did not block original binding sites for transporter or D2 receptor, but it significantly accelerated the washout of the tracer ligand (11C-CFT or 11C-raclopride) decreasing the binding potential.

# Calbindin Immunoreactivity in the striatum of a Normal Rat

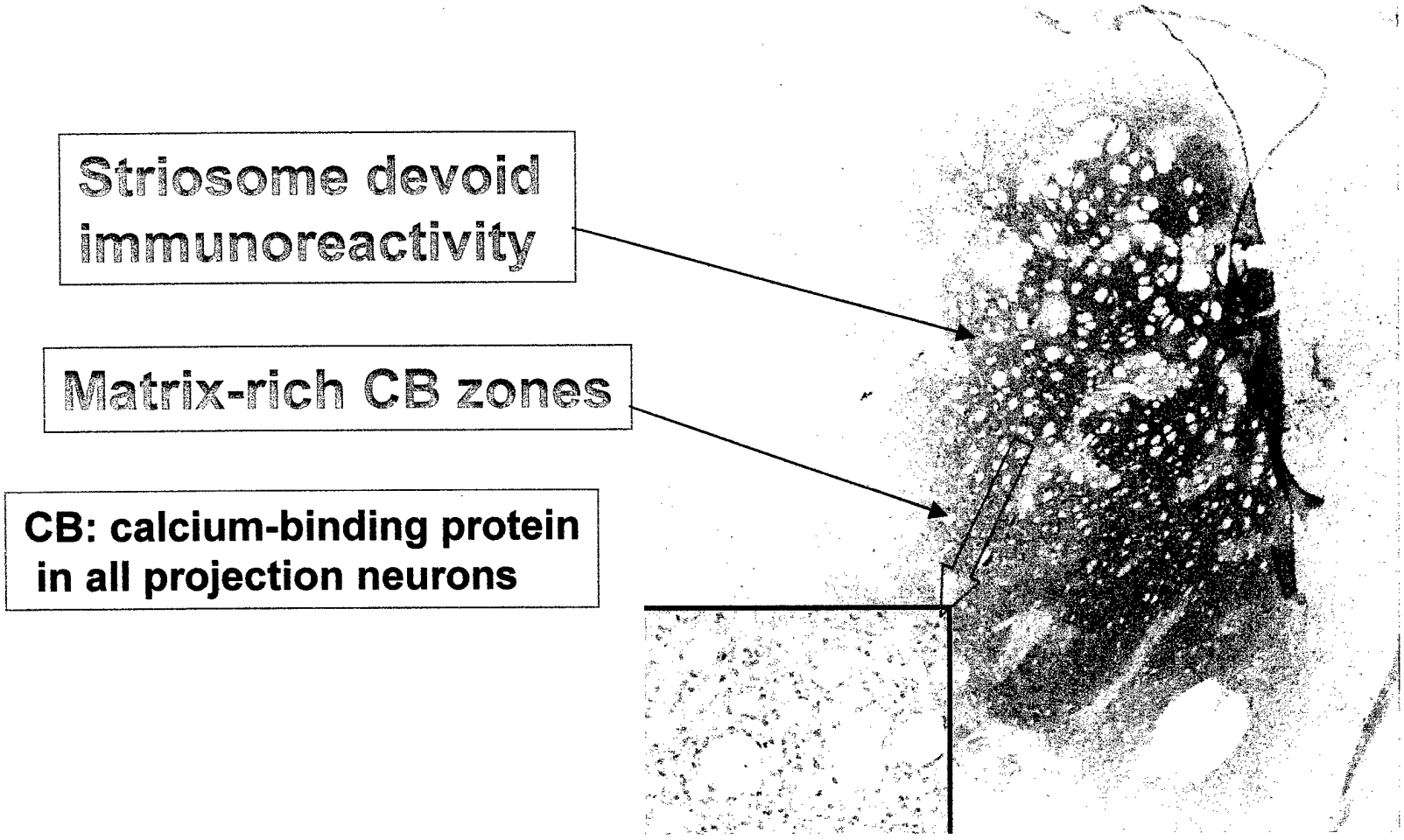


Figure 8. Low power photomicrographs of calbindin (CB) immunostaining in the striatum of a normal control animal. Note the patchy immunostaining intensity clearly depicting the striosome/matrix compartments of the striatum, typical of the CB staining. The inset illustrates a higher power magnification of striatal CB neurons in a healthy animal.

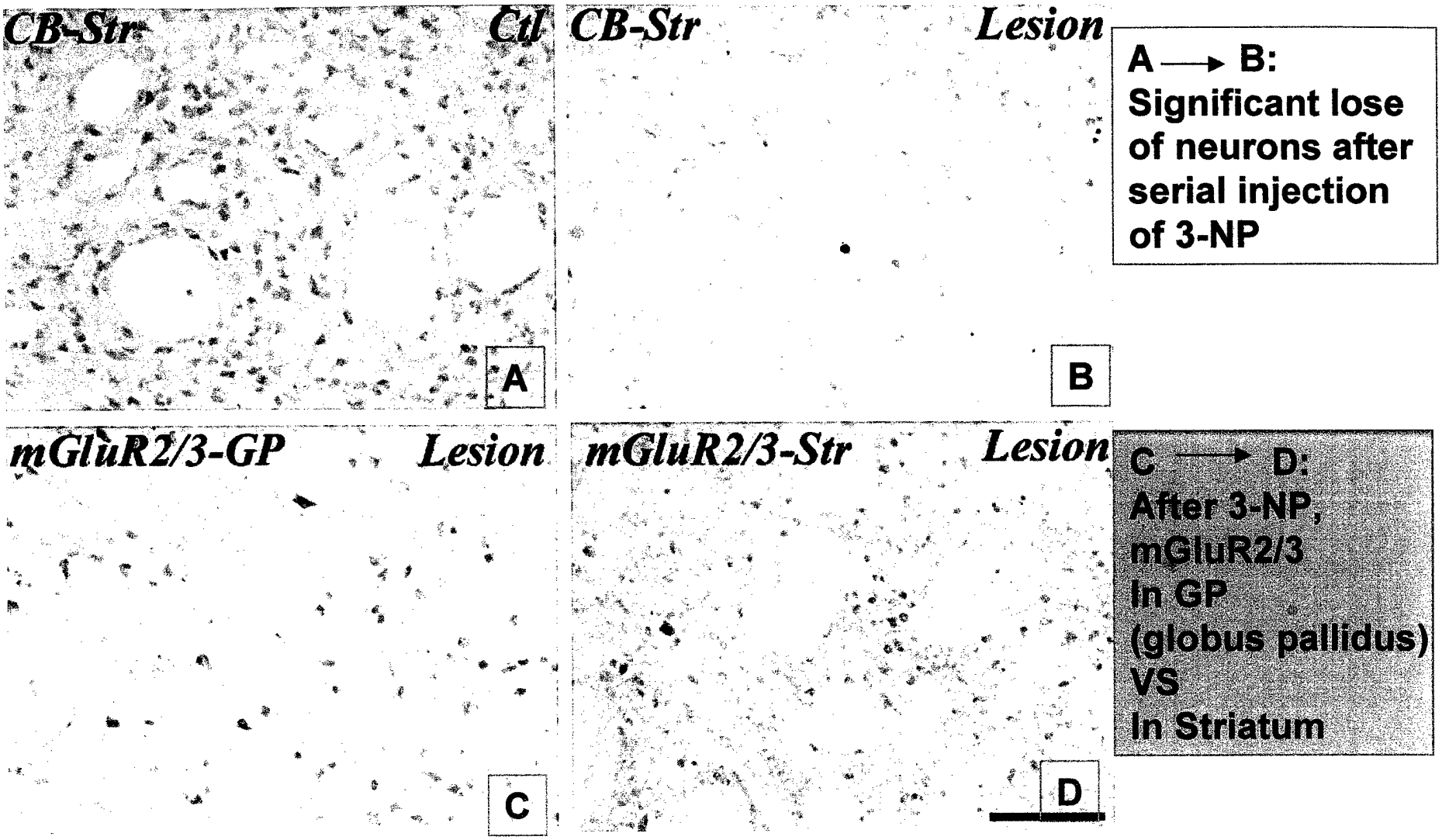


Figure 9. High power photomicrographs depicting CB immunostaining in a protected (ABHxD-I and 3NP treated) animal (top left; signed control) versus an animal, which underwent only 3-NP toxin treatment. Both pictures were taken in the striatum. Note the numerous healthy neurons in the protected animal (top left) compared to the smaller, unhealthy and sparsely distributed CB positive neurons of the lesioned animal. The expression of mGluR2/3 was also greatly affected by the infusion of only 3-NP in the striatum of these animals (bottom, right). In the other brain areas of the same 3-NP only lesioned animals, like the globus pallidus (bottom left), mGluR2/3 immunostaining revealed numerous cells expressing the receptor with no sign of ongoing degeneration. This also demonstrates that 3-NP toxicity has local affects in the brain.

# HIGH RESOLUTION IMAGING IN SMALL ANIMALS:
## Instrumentation, Applications and Animal Handling

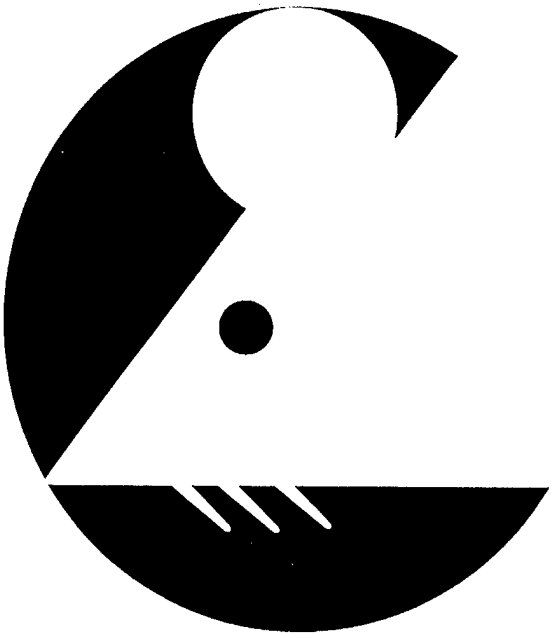

# PROGRAM-ABSTRACTS

SEPTEMBER 9–11, 2001
DoubleTree Hotel
Rockville, Maryland, USA

#162

**Glucose Utilization Assessed by High Resolution PET with Comparison to MRI/MRS in a Transgenic Mouse Model of Huntington's Disease**

Anna-Liisa Brownell[1], Y. Iris Chen[2], Kelly Canales[1], Robert Powers[1], Ole Andreasson[3], Flint Beal[3], and Bruce Jenkins[2]. Departments of [1]Radiology and [3]Neurology, Massachusetts General Hospital, Boston; [2]NMR Center, Massachusetts General Hospital, Charlestown.

**Summary**: We conducted longitudinal studies of glucose utilization and neurochemicals in a transgenic mouse model of Huntington's disease (HD) and littermate controls using high resolution PET and MRI/MRS techniques. Glucose is a sensitive marker of tissue energy metabolism, N-acetylaspartate (NAA) is a marker of neuronal health and choline (Cho) may be an indicator of gliosis. In the striatum of HD mice, a progressive linear decrease of glucose utilization and an exponential decrease in NAA was observed. The percent decrease in striatal NAA (compared to the wild-type animals) was two times higher than the percent decrease in glucose utilization. These observations parallel with the development of HD symptoms. In conclusion, this transgenic mouse model provides an excellent model for efficient study of human disease and high resolution in vivo imaging techniques provide unique quantitative approach to investigate pathophysiological processes in small animal models.

**Introduction**: After discovery of gene related diseases and development of different animal models to mimic the human diseases, a lot of pressure has come to develop in vivo imaging techniques, first to develop diagnostic methods to investigate pathophysiological processes and second to develop therapies for them. Recent advances in molecular engineering provide a direct animal link between human disease and transgenic mouse models to study pathophysiologic parallels and human-like response in transgenic mice. We investigated a transgenic mouse model of Huntington's disease. HD is an autosomal dominant inherited neuropsychiatric disease that usually starts at middle age and inevitably leads to death. The disease mutation consists of an unstable expanded glutamine trinucleotide repeat, coding region of the gene that encodes a stretch of polyglutamines. In humans, repeat length of >70 produce juvenile onset of HD. We used a transgenic mouse model of 82 CAG repeat. These mice develop normally, but about 6 weeks of age they show loss of brain and body weight, and around 9–11 weeks, develop many of the features of juvenile HD.

With newly developed high resolution in vivo imaging techniques it is possible to obtain information of the progression of the degeneration in different brain areas. This information is essential in evaluating overall pathophysiological processes as well as in developing therapies.

We have at the Massachusetts General Hospital, a long standing strong instrumentation development program accompanied with special software development program for special needs. These tools have been fundamental to develop applications in small animal models. PET studies in this application were done with an ultra high resolution in house built single ring PET scanner (resolution 1.3 × 1.3 × 1.8mm, 3.0 μl) connected to computer controlled imaging table. MRI/MRS studies were done with GE Omega 4.7 T imager.

**Methods**: We did PET imaging studies of glucose utilization and MRS studies of neurochemicals including N-acetylaspartate and choline in 30 transgenic mice with 82 CAG repeat and in 8 littermate controls. Imaging studies were conducted when the mice were 80–130 days old. For imaging studies mice were anesthetized using halothane (1.5–2.5% with oxygen flow rate of 1.5 L/min) and adjusted into a house built stereotactic head frame. For PET studies tail vein and artery were catheterized for administration of radioactivity and getting blood samples. Catheters were prepared of pediatric polyethylene tubing PE 10 (diameter of .011") and a needle size of 30G. Glucose concentration was determined of arterial blood and/or mixed venous and arterial blood of cut tail tip. After injection of $^{18}$F-fluorodeoxy-D-glucose (2FDG) (2–3 mCi) dynamic data were acquired for 20 min at the midlevel of heart and brain sequentially moving the imaging table back and forth between the two sites to obtain data of washout of radioactivity from blood and accumulation into the brain. The blood input function can be

detected of the tiny region of interest located inside the left ventricle. However, this data include spillover of the radioactivity accumulated in the heart muscle. To correct for this spillover 4 blood samples were taken from the cut tail tip between 1 and 20 min. When the steady state of radioactivity was reached, sequential scanning over the brain was done using 1.25 mm steps. Data were corrected for uniformity, sensitivty, and attenuation and images were reconstructed using Hanning filtered convolution backprojection with cut off value of 1.0. PET data were corrected for acquisition time, decay and injected dose and images were fused with MR images and volumetric region of interest including striatum and motor cortex were drawn based on MRI and anatomical atlas. Average radioactivity per voxel was calculated in striatum and motor cortex. Glucose metabolic rate was calculated using the Sokoloff model and a value 0.5 for the lumped constant.

In vivo MRS was acquired using a PRESS sequence and TR of 2000ms and three TE values (68, 136, and 272 ms). Voxels were placed symmetrically over both basal ganglia (average size of 6×3.5×3 mm, 63μl) or over the motor cortex (6×2×3mm, 36μl). Spectra were analyzed using the NMR1 software program (New Methods Research, Syracuse, NY). Spectra were integrated and normalized to the creatine/phosphocreatine peak.

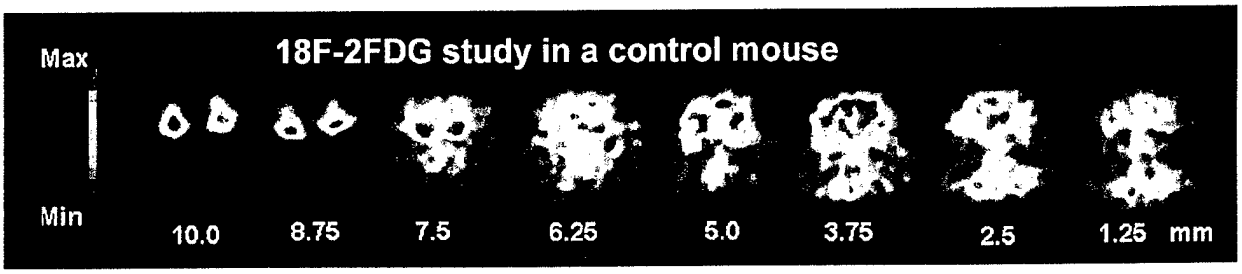


**Results**: Above is an image of 2FDG distribution in 8 coronal brain levels in a littermate control mouse. Longitudinal analyses of glucose utilization in HD mice showed in striatum a progressive decrease of 0.05%/day. The decrease in striatal NAA was one order higher being 0.56%/day. In the same time period Cho was increased 34% compared to littermate control. These observations parallel the developing of HD symptoms. Interestingly, no significant changes were found in cortical metabolism.

**Discussion**: In vivo high resolution quantitative imaging techniques can provide longitudinal information of multiple simultaneous processes in natural biological environment. This is the most important factor compared to in vitro techniques, which can provide brief information of isolated biological problems ignoring biological interaction created by the surrounding tissues and elements. These preliminary studies of glucose utilization and neurochemicals in a transgenic mouse model of Huntington's disease clearly demonstrate that this transgenic mouse model provides an excellent model for efficient study of human disease.




**Edit Menu** (Click on these to edit the data in your abstract.)

- Total characters left: **22**
- When you are satisfied that all the information below is complete and accurate, yo press the Save Abstract button to save your abstract so that you may return and co editing it at a later time. Remember that you must submit by the deadline for your to be considered.
- If you are ready to submit your abstract, you may press the Submit Abstract butto the submission payment screen and enter your credit card information. You must submission fee for your abstract to be considered.
- Submission of this abstract is final, like putting a paper abstract into the mailbox. have submitted and paid for your abstract, you will not be able to revise it without submitting a replacement abstract and paying the replacement abstract fee of $50.
- If you are going to submit this abstract, be sure to print this page for your records.
- After you have submitted your abstract, and received your control number, you m contact the SFN Program Department if you wish to have your abstract withdrawn

**To see a sample of what your abstract will look like, click** ere.

**Contact Info**
Anna-Liisa Brownell
Massachusetts General Hosp
Boston
MA 02114
USA
Phone: 617-726-3807
Fax: 617-726-5123
abrownell@partners.org

**Date/Time Last Modified:** 04/23/2001 at 3:02 pm

**Presentation Type:** Slide/Poster

**Theme 1:** Neurological and Psychiatric Conditions

**Subtheme 1:**

**Topic 1:**

**Theme 2:** Neurological and Psychiatric Conditions

**Subtheme 2:**

**Topic 2:**

**Abstract Title:** 3-NP INDUCED NEUROTOXICITY - ASSESSED BY ULTRA RESOLUTION PET WITH COMPARISON TO MRI AND MRS

**Contributing Authors:** A.-L. Brownell[1*]; Y.I. Chen[1]; K.E. Canales[1]; E. Livni[1]; R.T. Pow Dedeoglu[2]; F.M. Beal[3]; B.G. Jenkins[1]

**Institutions:** 1. Radiology, 2. Neurology, Massachusetts General Hosp, Boston USA

3. Neurology, Cornell University Medical School, New York, N

# 3-NP induced neurotoxicity - assessed by ultra high resolution PET with comparison to MRI and MRS

A-L Brownell, YI Chen, KE Canales, RT Powers, A Dedeoglu, FM Beal, BG Jenkins,

3-NP, a succinate dehydrogenase inhibitor, is widely used as an experimental model to study HD, energy metabolism and cell death. We used a rat model to investigate 3-NP induced acute and prolonged neurotoxicity using in vivo imaging of cerebral glucose utilization (CGU)and dopamine receptors by PET, neuroanatomy by MRI and neurochemicals by MRS. 3-NP was administered (male Spraque-Dawley) twice a day (10 mg/kg ip.) until symptomatic or max of 5 days. PET studies of CGU were conducted daily using a super high resolution (1.3x1.5x1.5 mm3) in-house built PET device. MRI and MRS studies were conducted with a GE Omega 4.7 T imager.

Studies of CGU showed significant interanimal variation in the acute response of toxin, similar to motor activity. The average decrease of CGU in the lesions was 31+/-12% and the lesions started to develop on the first day of 3-NP. Four weeks later CGU was recovered to -13+/-5% and then in 3 months decreased again to –48+/-10%. Dopamine D1 and D2 receptors showed progressively decreasing binding by PET after 3-NP using 11C-SCH and 11C-raclopride, respectively. However, the binding of dopamine transporter imaged by 11C-CFT showed early increase (1 week after 3-NP) followed by progressive decrease. MRS showed elevated peaks of lactate and macromolecules as well as succinate immediately after 3-NP toxicity which diminished in 4 months, indicating a reversible process. Choline peak increased and N-acetylaspartate peak decreased in 4 months indicating loss and damage of neurons. Post mortem histological studies confirmed the neural loss.

The Society for Molecular Imaging™

SIEMENS medical

PHILIPS

GE Medical Systems

THE DANA FOUNDATION

NATIONAL CANCER INSTITUTE

The Journal for Molecular Imaging™

**First Annual Meeting**
**of the Society for Molecular Imaging**
August 24-26, 2002
Boston Long Wharf Marriott

Please note: This registration site has a time out period of 30 minutes. If y an abstract, we recommend you compose it elsewhere and paste it int

YOUR REGISTRATION IS NOT COMPLETE UNTIL YOU HAVE COMPLETED A TINAL CONFIRMATION PAGE WILL INCLUDE YOUR REGISTRATION CODE, P CODE AS YOUR CONFIRMATION RECEIPT. YOU WILL ALSO NEED IT TO EDI REGISTRATION.

## Abstract Submission

Abstracts submited by Anna-Liisa Brownell

1 [redacted]

- Click title to view or edit abstract
- Save current to start new abstract
- Save blank title to remove abstract

**Deadline to submit abstracts is June 3.**

Please Note: this will appear in program exa on this page.

Title
3-NP induced neurotoxicity- assessed by P

Author(s)
A-L. Brownell, Y.I. Chen, M. Yu, B.G. Jenki

List first 4 with et al., First initials and last name, no f out.

Affiliation: **Massachusetts General Hospital** Department: **Radiology**

Category Neurobiology

No figures or references should be listed on

Abstract 2000 Characters Left (250 Word

3-Nitropropionic acid (3-NP), a succinate dehydrogenase inhibitor, is widely used as experimental model to study Huntington's

**Abstract View**

## 3-NP INDUCED NEUROTOXICITY - ASSESSED BY ULTRA HIGH RESOLUTION PET WITH COMPARISON TO MRI AND MRS

[redacted] ; [redacted] ; [redacted] ; [redacted] ; [redacted] ; [redacted] ; [redacted] ;

*1. Radiology, 2. Neurology, Massachusetts General Hosp, Boston, MA, USA*

*3. Neurology, Cornell University Medical School, New York, NY, USA*

3-NP, a succinate dehydrogenase inhibitor, is widely used as an experimental model to study HD, energy metabolism and cell death. We used a rat model to investigate 3-NP induced acute and prolonged neurotoxicity using in vivo imaging of cerebral glucose utilization (CGU)and dopamine receptors by PET, neuroanatomy by MRI and neurochemicals by MRS. 3-NP was administered (male Spraque-Dawley) twice a day (10 mg/kg ip.) until symptomatic or max of 5 days. PET studies of CGU were conducted daily using a super high resolution (1.3x1.3x1.8 $mm^3$) in-house built PET device. MRI and MRS studies were conducted with a GE Omega 4.7 T imager.
Studies of CGU showed significant interanimal variation in the acute response of toxin, similar to motor activity. The average decrease of CGU in the lesions was 31+/-12% and the lesions started to develop on the first day of 3-NP. Four weeks later CGU was recovered to -13+/-5% and then in 3 months decreased again to -48+/-10%. Dopamine D1 and D2 receptors showed progressively decreasing binding by PET after 3-NP using $^{11}$C-SCH and $^{11}$C-raclopride, respectively. However, the binding of dopamine transporter imaged by $^{11}$C-CFT showed early increase (1 week after 3-NP) followed by progressive decrease. MRS showed elevated peaks of lactate and macromolecules as well as succinate immediately after 3-NP toxicity which diminished in 4 months, indicating a reversible process. Choline peak increased and NAA peak decreased in 4 months indicating loss and damage of neurons. Post mortem histological studies confirmed the neural loss.
*Supported by: DAMD17-99-1-9555*

close

The 49th
Society of Nuclear Medicine
Annual Meeting

ABSTRACT BOOK

Scientific Abstracts of
the 49th Annual Meeting of
the Society of Nuclear Medicine
Los Angeles, CA • June 15-19, 2002

No. 859

**NEW APPROACHES IN PARAMETRIC IMAGING - USE OF DIRECT ALGORITHM.** K. Canales*, A. Brownell, Massachusetts Institute of Technology, Cambridge, MA; Department of Radiology, Massachusetts General Hospital, Boston, MA. (202189)

**Objectives:** Generation of parametric images requires the fitting of a tracer-kinetic model to time activity curve data from dynamic image sequences on a voxel-by-voxel basis. The parametric image computed results in a quantitative image that depicts the values of a certain rate depending on the physiological or biochemical model employed. Many algorithms have been developed in previous years for generating parametric images. These algorithms differ in their generality, computational speed and performance. The DIRECT algorithm developed by Jones, Perttunen, and Stuckman has proven useful for optimizing the noisy function values typical of realistic simulations in large-scale engineering designs. We used this algorithm to generate parametric images of receptor-radioligand binding in dynamic PET image sequences reconstructed by convolution backprojection and Bayesian MAP routines. **Methods:** PET images of radioligand-receptor binding using both $^{11}$C-raclopride and $^{11}$C-CFT from four male monkeys (Macaca fascicularis) both before and after MPTP treatment were used in this study. Image data was first corrected for uniformity, sensitivity, and attenuation. Image data was then reconstructed, first using Hanning weighted convolution backprojection, then using Bayesian MAP. The reconstructed data was then filtered and decay corrected; and parametric images of k1, k2, k3, k4 and Bmax/Kd using a two tissue compartmental model were generated using an implementation of the DIRECT algorithm. ROI analysis of the parametric images were used to obtain values over specific regions of interest and then compared to standard compartmental modelling results. **Results:** Values from parametric images generated by the algorithm for $^{11}$C-raclopride and $^{11}$C-CFT corresponded reasonably well to standard compartmental analyses. The values of Bmax/Kd for raclopride generated from parametric imaging were within $90+/-6\%$ of the values reported from standard compartmental analyses; and values from all methods were well within the range of expected results for these type of studies. **Conclusions:** The DIRECT algorithm provides an efficient, easy-to-implement, routine for the generation of parametric images.

The 49th
Society of Nuclear Medicine
Annual Meeting

ABSTRACT BOOK

Scientific Abstracts of
the 49th Annual Meeting of
the Society of Nuclear Medicine
Los Angeles, CA • June 15-19, 2002

No. 220

## NEURAL DEGENERATION IN A TRANSGENIC HD MOUSE MODEL — AN ULTRA HIGH RESOLUTION PET STUDY WITH COMPARISON TO MRI/MRS.

A. L. Brownell*, Y. I. Chen, K. Canales, B. Powers, B. G. Jenkins, Massachusetts General Hospital, Boston, MA. (202010)

**Objectives:** Recent advances in molecular engineering provide a direct animal link between human disease and transgenic mouse models to study pathophysiological parallels. We investigated a transgenic mouse model of Huntington's disease (HD). The disease mutation consists of an unstable expanded glutamine trinucleotide repeat. In humans, repeat length of >70 produces juvenile onset of HD. We used a transgenic mouse model, repeat length of 82. **Methods:** PET imaging studies of glucose utilization using ulta-high resolution tomograph with inplane resolution of 1.16mm X 1.16mm and MRS studies of neurochemicals including N-acetylaspartate (NAA) and choline (Cho) were conducted in 34 transgenic mice and 10 littermate controls. Imaging studies were started when mice were 70 days old and continued until their death. The lifespan is about 130 days. For imaging studies mice were anesthetized with halothane (1.5-2.5% with oxygen flow of 1.5 L/min). For PET studies tail vein and artery were catheterized for injection of activity (2 mCi $^{18}$F-FDG) and obtaining of blood samples for quantitation. Dynamic data were acquired for 20 min. Sequential imaging over the brain was done using 1.25 mm steps. In vivo MRS was done using a 4.7T Omega CSI spectrometer and a PRESS sequence with TR of 2000ms and three TE values (68,136, and 272 ms). Voxels were placed symmetrically over the basal ganglia and motor cortex. Obtained spectra were integrated and normalized to the creatine/phosphocreatine peak. **Results:** Longitudinal analysis of glucose utilization in HD mice showed in striatum a progressive decrease of 0.05%/day. The decrease in striatal NAA was one order higher being 0.56%/day. In the same period Cho increased 34% compared to littermate controls. These observations parallel with the developing HD symptoms. **Conclusions:** These preliminary studies of glucose metabolism and neurochemicals in a transgenic mouse model of HD clearly demonstrate that this transgenic mouse model provides an excellent model for effective study of human disease.

The 49th
Society of Nuclear Medicine
Annual Meeting

ABSTRACT BOOK

Scientific Abstracts of
the 49th Annual Meeting of
the Society of Nuclear Medicine
Los Angeles, CA • June 15-19, 2002

No. 397

**METABOTROPIC GLUTAMATE RECEPTORS - NEW TARGETS FOR NEUROIMAGING.** A. Brownell*, K. Canales, Y. I. Chen, C. Owen, R. Powers, A. Kozikowski, D. Elmaleh, M. Yu, Massachusetts General Hospital, Boston, MA; Massachusetts Institute of Technology, Cambridge, MA; Georgetown University, Washington, DC. (201766)

**Objectives:** Glutamate is the most abundantly active neurotransmitter in the mammalian brain and mediates the excitatory pathways in mammals. However, the lack of specific antagonists has limited the precise characterization of the role of individual metabotropic glutamate receptors (mGluRs) in glutamatergic neurotransmission and has hampered progress in identifying the physiological and pathological roles of mGluRs. **Methods:** PET studies were conducted in the brain of control and MPTP induced primate Parkinson's disease model to investigate regional distribution of $^{11}$C labeled methyl 2-(methoxycarbonyl)-2-(methylamino) bicyclo(2.1.1)-hexane-5-dicarboxylate (MMMHC). MMMHC passes BBB and will be metabolized to 2-aminobicyclo(2.1.1)hexane-2,5-dicarboxylic acid-I, a potent mGluR2 agonist. Primates were injected with 10 mCi of the $^{11}$C-MMMHC. Dynamic data were acquired for 90 min with PCR-I, an in-house built tomograph and arterial blood samples were drawn to determine input function. In the same primates, dopamine transporters were investigated with $^{11}$C-CFT and dopamine D2 receptors with $^{11}$C-raclopride. In addition, studies of cerebral blood flow and oxygen metabolism were done using the steady state inhalation technique. **Results:** $^{11}$C-MMMHC showed in the MPTP treated monkey 39% decrease in binding potential (BP) in the basal ganglia, 45% in the visual, 44% in the motor and 56% in the temporal cortex, respectively. $^{11}$C-CFT showed 52% decrease in striatal dopamine transporter binding and 15% elevated D2 receptor binding. No significant changes were observed in studies of blood or oxygen metabolism. **Conclusions:** $^{11}$C-MMMHC binds in the normal brain to the sites which are rich of mGluRs. This binding pattern is significantly affected after MPTP neurotoxicity indicading that in addition to dopaminergic system also glutamatergic system is involved in MPTP induced neural degeneration.

The 49th
Society of Nuclear Medicine
Annual Meeting

ABSTRACT BOOK

Scientific Abstracts of
the 49th Annual Meeting of
the Society of Nuclear Medicine
Los Angeles, CA • June 15-19, 2002

No. 609

**$^{11}$C LABELLING OF METHYL 2-(METHOXYCARBONYL)-2-(METHYLAMINO) BICYCLE (2.1.1)-HEXANE-5-CARBOXYLATE, A POTENT NEUROPROTECTIVE DRUG.** M. Yu*, E. Livni, K. Nagren, K. Canales, R. Powers, D. Elmaleh, A. Kozikowski, A. L. Brownell, Department of Radiology, Massachusetts General Hospital, Boston, MA; Turku PET Centre, Turku, Finland; Georgetown University Medical Center, Washington, DC. (201330)

**Objectives:** If energy metabolism is compromised, glutamate (Glu) may act as a neurotoxin. The neurons in many neurologic disorders may be injured at least partly by over stimulation of Glu receptors. Metabotropic glutamate receptor (mGluR) Group II agonists have demonstrated neuroprotective effects in vivo. 2-aminobicyclo[2.1.1]-hexane-2,5-dicarboxylic acid –I (ABHxD-1) is a potent mGluR2 agonist with $EC_{50}$ 0.33$\mu$M with neuroprotective effects in vitro, but it is unlikely to pass the BBB. A new ABHxD-1 analog, methyl 2-(methoxycarbonyl)-2-(methylamino) bicyclo[2.1.1]-hexane-5-carboxylate (MMMHC), was synthesized from ABHxD-1. It passes BBB and may be metabolized to ABHxD-1 by enzymes in the brain and result in neuroprotection. We labelled MMMHC with C-11 to evaluate its brain distribution by PET. **Methods:** 0.10 mg free base precursor (methyl 2-(methoxycarbonyl)-2-amino bicyclo[2.1.1]-hexane-5-carboxylate) in 100 $\mu$ l acetone was used to trap C-11 methyl triflate at 0°C, then it was heated at 60°C 1 min. After purification by HPLC, the collected fraction was evaporated and dissolved in saline. After sterile filteration, it was used in experimental studies. **Results:** The C-11 labelling yield was 69%, the radiochemical purity was over 99%, more than 100 mCi product was available in 40 min (EOB). The C-11 MMMHC accumulates fast into the brain and binds mainly in cortex. Accumulation in different cortical areas in primate brain was 3.0-4.8%ID/100cc, at 40 min after injection of the ligand. At the same time accumulation in the basal ganglia was 4.1-4.7%ID/100cc. **Conclusions:** The compound MMMHC can be labelled with carbon-11 with its free base precursor. In vivo study showed that the MMMHC compound passes the BBB and bound in cortical sites which are rich of group II metabotropic glutamate receptors.

**Neurotoxicity (3-NP) induced changes in striatal dopamine receptor function.**

Anna-Liisa Brownell, Iris Y. Chen, Xukui Wang, Meixiang Yu, Bruce G. Jenkins
Radiology, Massachusetts General Hospital, Boston, MA

Striatal dopaminergic system is vulnerable to many neurotoxic agents, like MPTP, which affects through complex I in the electron transport chain. We investigated short-term and long-term effects of 3-NP induced neuroxicity in sriatal dopamine receptor function. 3-NP affects through complex 2. The initial insult of both MPTP and 3-NP is impairment of ATP production. We conducted PET imaging studies of dopamine D1 and D2 receptors and dopamine transporters in 12 rats (Spraque Dawley, male) before 3-NP injections and 2 days, 4 weeks and 4 months post 3-NP. Dopamine D1 receptors were imaged with $^{11}$C-SCH (Schoering 23660) and dopamine D2 receptors with $^{11}$C-raclopride. Dopamine transporters were imaged with $^{11}$C-CFT (2β-carbomethoxy-3β-4-fluorophenyl tropane). Because of the inter animal variation of the response of 3-NP toxicity, a study of glucose metabolism was conducted 2 days after 3-NP to estimate brain damage. Small decreases in dopamine D1 and D2 receptor bindings (4+/-2 % and 5+/-2 %, respectively) were observed 2 days after 3-NP. In 4 weeks, more severe decreases were observed (-24+/-8 % and -23+/-7 %, correspondingly). After that gradual depletion of dopaminergic system continued and 4 months later dopamine D1 and D2 receptor binding was (36+/-9 and 33+/- 8 % correspondingly). Interestingly, dopamine transporter binding imaged by $^{11}$C-CFT showed early increase 2 days after 3-NP administrations (6+/-3%). After that moderate decrease was observable: -10+/-3% in 4 weeks and -12+/-4% in 4 months. These experiments demonstrate that striatal dopamine receptor function is modulated also by neurotoxin affecting through complex 2. However, the damage is more prominent in the postsynaptic site than in the presynaptic site.

Parkinson's disease: The Life Cycle of the Dopamine Neuron

Anna-Liisa Brownell, Ph.D.
Associate Professor
Bartlett Hall 504R
Radiology
Massachusetts General Hospital
Boston, MA 02114

Tel: 617-726-3807
Fax: 617-726-5123
Email: abrownell@partners.org

# MAPPING OF BRAIN FUNCTION AFTER MPTP INDUCED NEUROTOXICITY IN A PRIMATE PARKINSON'S DISEASE MODEL

Anna-Liisa Brownell[1,2], Kelly Canales [1], Y. Iris Chen [1], Bruce G. Jenkins[1], Christopher Owen[3], Elijahu Livni [1], Meixiang Yu[1], Francesca Cicchetti [2], Rosario Sanchez-Pernaute [2], Ole Isacson [2, 4]

[1]Radiology, [3] Neurosurgery, [4]Neurology, Massachusetts General Hospital, Boston, MA 02114, [2]Udall Parkinson's Disease Research Center of Excellence, Neuroregeneration Laboratory, McLean Hospital, Belmont, MA 02478

Running title: Mapping of brain function
Key words: positron emission tomography, volume rendering, MPTP, Parkinson's disease

Correspondence to:
Dr. Anna-Liisa Brownell
Department of Radiology
Massachusetts General Hospital
Bartlett Hall 504R
Boston, MA 02114
Phone: 617-726-3807
Fax; 617-726-5123
Email:abrownell@partners.org

**Summary**

Neurophysiological studies of the brain in normal and Parkinson's disease patients have indicated intricate connections for basal ganglia induced control of signaling into the motor cortex. To investigate if similar mechanisms are controlling function in the primate brain (Macaca fascicularis) after MPTP induced neurotoxicity, we conducted PET studies of cerebral blood flow, oxygen and glucose metabolism, dopamine transporter and D2 receptor function. An Actiwatch was used to record behavioral locomotor activity in primates. For PET data analyses we developed topographic mapping of the brain based on volume rendering and co-registration (fusion) of PET and T2 weighted MRI data.

Our observations after MPTP induced dopamine terminal degeneration of the caudate and putamen revealed increased blood flow (15%) in the globus pallidus (GP), while blood flow was moderately decreased (15-25%) in the other brain areas, including caudate, putamen, thalamus and substantia nigra (SN). In the primary motor cortex (PMC), blood flow was decreased by 40%. Oxygen extraction fraction was moderately increased (10-20%) in all brain areas; and oxygen metabolism was significantly increased in the GP, SN and SMA by a range of 20-40%. Decreases in oxygen metabolism were observed in the putamen and caudate and in the PMC. Similarly, decreases were observed in glucose metabolism in the caudate, putamen, thalamus and PMC (range 35%- 50%). However, glucose metabolism was enhanced in the GP by 15%, and no change was observed in the SMA. In the parkinsonian primate, $^{11}$C-CFT (2β-carbomethoxy-3 β -(4-flurophenyltropane) dopamine transporter binding was significantly decreased in the putamen and caudate (range 60-65%). $^{11}$C-raclopride binding of dopamine D2 receptors did not show significant total change.

These results parallel observations made in Parkinson's disease patients. We conclude that, in spite of decreases in global cerebral energy metabolism after MPTP induced dopamine terminal degeneration, elevated blood flow, oxygen consumption and glucose utilization occur in the GP as well as the SMA, which is part of a compensatory functional mechanism obtained by changes in the neural motor circuitry.

## Introduction

Parkinson's disease (PD) is characterized neuropathologically by a severe depletion of DA neurons and an associated loss of axons and terminals in the basal ganglia (Kish et al., 1988). Diagnosis is based on clinical signs of tremor, rigidity, bradykinesia and postural instability (Marsden, 1992).

Hypotheses of the etiology of PD focus on the potential contribution of environmental toxins (exogenous and/or endogenous) and their interactions with genetic components (Checkoway and Nelson, 1999; Gorrell et al., 1996; Mizuno et al., 1999; Schapira, 1996). Cell death introduced by toxins may trigger a cascade of biological processes with an endpoint of continuous degeneration (Brownell et al., 1998; Brownell et al., 1999; Schmidt and Ferger, 2001). These biological processes affect primarily the dopaminergic system in the basal ganglia and the neural network of the motor system (Alexander et al., 1986; Alexander et al., 1990; Wichman and DeLong, 1996; DeLong and Wichman, 2001).

MPTP (1-methyl-4-phenyl-1,2,5,6 tetrahydropyridine) neurotoxicity has long been used as a model for Parkinson's disease because it induces dopaminergic cell death in the substantia nigra pars compacta and striatal dopaminergic degeneration (Palombo et al., 1991; Schmidt and Ferger, 2001). MPTP induced dopaminergic degeneration causes decreases in the binding of presynaptic dopamine transporters and reduces locomotor activity (Hantraye et al., 1992; Wullner et al., 1994).

A number of *in vivo* imaging studies in PD patients have shown regional differences in glucose metabolism and blood flow (Brooks, 2001; Eidelberg et al., 1995b; Fukuda et al., 2001; Markus et al., 1995). These studies show that glucose utilization and cerebral blood flow reductions in the brain correlate with the severity of the disease (Berding et al., 2001; Eberling et al., 1994; Eidelberg et al, 1995a; Moeller and Eidelberg, 1997; Imon et al., 1999). Antonini et al have even proposed that studies of glucose metabolism can be used for differential diagnosis of PD (Antonini et al., 1998).

There is, however, great variability in the reports of absolute values of local metabolic functions (Antonini et al., 1995; Bohnen et al., 1999; Eberling et al., 1994).

This may originate from methodological differences during imaging studies, variability in the resolution of the imaging devices and, finally, differences in the selection of regions of interest, as well as level of degenerative process. Eidelberg and Brooks have used a statistical parametric mapping technique with normalized values to evaluate metabolic changes in different brain areas in PD patients before and after therapeutic regimen (Brooks, 2001; Eidelberg et al., 1996). Autoradiographic studies in primates (Palombo et al., 1990; Porrino et al., 1987) have shown significant local changes in glucose utilization in basal ganglia, cerebral cortex and cerebellum after MPTP.

Based on neurophysiological experiments four different loops have been characterized to control signaling between the basal ganglia and the cortex (Alexander et al., 1990). In PD, the most sensitive loop is between the putamen, globus pallidus, thalamus and cortex. The motor loop links the supplementary motor area (SMA) to the primary motor cortex, dorsal putamen, pallidum and ventrolateral thalamus, while the dorsolateral prefrontal cortex loop links dorsal caudate and ventroanterior thalamus (Isacson et al., 2001). Studies in PD patients have postulated that the nigrostriatal DA deficiency leads to decreased inhibition of the internal segment of the globus pallidus by both direct and indirect pathways (Alexander et al., 1990). Resulting excessive inhibitory output from the globus pallidus suppresses the ventral thalamus, reducing activation of the supplementary motor area and prefrontal cortex, and creates the motor impairments characteristic of PD (Alexander, 1987; Crutcher and DeLong, 1984; Wichman and DeLong, 1996). Cerebral blood flow activation studies have been conducted to investigate these neural control mechanisms using different behavioral tasks in awake patients (Samuel et al, 1997; Brooks, 2001).

To investigate if similar neural circuitry linked mechanisms are operating in primate models of parkinsonism induced by MPTP, we conducted experimental imaging studies before and after MPTP of cerebral blood flow, oxygen extraction fraction, oxygen and glucose metabolism, dopamine transporters and dopamine D2 receptors using positron emission tomography (PET). All experimental studies of neural function were conducted in anesthetized primates.

For data analyses, a volumetric technique was developed to select regions of interest based on both a primate brain atlas and actual MRI data. PET data were co-

registered with the complete brain volume of MR data, and the resulting volumetric-PET data were used for quantitative data analyses.

## Methods

### *Procedures in primates*

Five male monkeys (Macaca fascicularis) were injected with MPTP (0.3 or 0.5 mg/kg iv. weekly) until PD symptoms appeared (Wullner et al., 1994). PET imaging studies were conducted before MPTP administrations and 2-3 months after cessation of MPTP. Additionally, 4 monkeys were used in control studies. For the imaging studies, primates were anesthetized using halothane (1.5% with oxygen flow rate of 3 L). Arterial and venous catheterization was done for drawing blood samples and injecting of labeled ligands. Animals were adjusted into a stereotactic head holder with ear bars at the origin. Interior orbital supports ensure that images are acquired on a pseudocoronal plane perpendicular to the orbito-metal line. This allows superposition of the data from MRI studies. Level of anesthesia, blood gases, heartbeat and vital signs were monitored throughout the imaging procedures (Propaq, "Vital Signs Monitor", Protocol Systems. Inc., Beaverton, Oregon, USA).

Imaging studies of blood flow and oxygen and glucose metabolism were conducted in one imaging session; and studies of dopamine transporters and $D_2$ receptors were conducted in another session within the time span of a week. The MRI studies, needed for anatomical data, were conducted within a month. This short time span is necessary to eliminate possible errors in volumetric data fusion, raised by neurotoxicity induced morphologic volumetric changes. Table I shows the number of the animal studied in each imaging category.

**Table I. Number of studies and primates used (studies/primates) in each imaging category.**

| | Blood flow | Oxygen metabolism | Glucose metabolism | Dopamine transporter | Dopamine D2 receptor |
|---|---|---|---|---|---|
| Control studies | 4/4 | 4/4 | 4/4 | 5/5 | 5/5 |
| After MPTP | 4/4 | 4/4 | 4/4 | 5/5 | 5/5 |

Animals used in this study were maintained according to the guidelines of the Committee on Animals of the Harvard Medical School and Massachusetts General Hospital and of the "Guide for Care and Use of Laboratory Animals" of the Institute of the Laboratory Animal Resources, National Research Council, Department of Health, Education and Welfare, Publication No. (NIH)85-23.

***Detection of locomotor activity***

Spontaneous locomotor activity was monitored by an Actiwatch system (Mini Mitter Company, Inc., Sunriver, OR) mounted in a shirt pocket in the back of the animal (Puyau et al., 2002). The Actiwatch reader was connected to a computer, and data were transferred from the Actiwatch to a computer through a wireless link. The Actiwatch allows analyses of circadian rhythms, average activity during light and dark, mean activity score, movement and movement type index. Prior to MPTP injections, there was a significant difference between day and night time locomotor activity, while after MPTP no activity difference was observable (Figure 1). The difference in locomotor activity was used as one criteria of parkinsonism.

***PET imaging***

PET imaging studies were conducted with an in-house-built single ring PET device, PCR-I (Brownell et al., 1989). Spatial resolution of the PET system is 4.5 mm and sensitivity 40kHz/μCi. Data acquisition over the whole brain volume with this single ring device was done stepwise using 5 mm thick coronal slices with 5 mm steps. Imaging

data were corrected for uniformity, sensitivity, attenuation, decay and acquisition time. PET images were reconstructed using a Hanning filtered convolution backprojection with a cut-off value of 1.0. Calibration of the positron tomograph was performed prior to each study using a cylindrical plastic phantom (diameter 6 cm) containing water solution of $^{18}F$. The corrected reconstructed data set was repacked on the Linux workstation and converted into ANALYZE/AVW image format. The voxel size in coronal PET images is 5 mm in the axial Z-direction and 1.19 mm x 1.19 mm in x-y plane.

After that T2 weighted MRI data from the same subject were loaded and converted into ANALYZE/AVW image format. A segmentation routine in ANALYZE was used to separate the brain from the surrounding tissue in the MRI data. PET data were then thresholded and co-registered to its respective MRI data using the NMI (Normalized Mutual Information) voxel match algorithm of the ANALYZE software package and cubic spline interpolation. A resulting transformation matrix maps the PET images onto its respective MR images, and the multimodality image registration routine returns fused PET-MRI images. The fused PET-MR images were then volume rendered for display (Figure 2).

***Selection of the volume of interest***

Three-dimensional regions of interest were outlined on coronal MR slices based on anatomical borderlines observed from primate brain atlas and MR images (Figure 3). These regions were also computationally compared and verified with the corresponding slices in primate brain atlas. The transformation matrix for fusing the PET data to the MRI data was then reapplied to the PET images to generate the data for three-dimensional VOI (volume of interest) analysis. Volumetric radioactivity concentration was calculated for each VOI; and these data were then used for further data analyses to calculate values for blood flow, oxygen extraction fraction and metabolism, glucose metabolism and binding potential for dopamine transporters and dopamine D2 receptors.

***Validation of the volumetric data analyses***

To validate the three-dimensional data analyses we conducted studies with a phantom consisting of two concentric spheres (Data Spectrum Corporation, Chapel Hill,

NC, USA). The volume of the inner sphere was 20 ml, and the volume of the outer sphere was 79 ml. In the first experiment the outer sphere was filled with $^{18}F$-labeled water, and the inner sphere was filled with water without radioactivity. The phantom was scanned stepwise with 5 mm steps (Figure 4). In the second experiment the inner sphere was filled with higher radioactivity concentration than in the outer sphere, which had the same radioactivity concentration as in the first experiment. Additionally, T2 weighted MR images were done with both concentric spheres filled with water. The data analyses were conducted in the same way as above by drawing ROIs on MR images and then fusing PET data with MRI data. Finally, radioactivity concentration was determined and compared with actual measured radioactivity. For comparison, radioactivity concentration was also calculated based on conventional 2-dimensional pixel analyses (Table II).

***Blood flow studies***

Blood flow studies were conducted using a steady state technique based on the inhalation of $C^{15}O_2$ (Frackowiak et al., 1980; Jones et al., 1976; Subramanyam et al., 1978). $^{15}O$ labeled $CO_2$ gas mixture was delivered at a constant concentration and flow rate (2L/min) into the inhalation tube. After 6-8 min of inhalation of $C^{15}O_2$ gas mixture, a steady state activity level was obtained in the brain; and sequential imaging over the brain was performed. During imaging, a series of arterial blood samples were drawn to determine blood gases and radioactivity in the plasma and whole blood. These data are needed for calculation of the oxygen extraction level (Subramanyam et al., 1978). Radioactivity was measured in a gammacounter (Packard Cobra Auto-gamma, Downers, IL, USA), which was cross-calibrated with the tomograph. Arterial blood and plasma radioactivity concentrations were then computed after corrections for dead time and decay.

***Studies of oxygen extraction fraction and metabolism***

After the blood flow study, the inhalation gas mixture was switched to $^{15}O_2$. In 10-12 min a steady state activity level was obtained in the brain based on stabilized

oxygen metabolism and blood flow (Jones et al., 1976; Subramanyam et al., 1978). A similar sequential imaging over the whole brain was performed as above. During imaging arterial blood was drawn to determine blood gases, hematocrite, hemoglobin and radioactivity levels in the plasma and whole blood. These data are necessary to calculate the oxygen extraction fraction (Jones, 1976; Subramanyam et al., 1978). Regional cerebral oxygen metabolism can be calculated when blood flow, oxygen extraction fraction, blood gases and hemoglobin are known (Subramanyam et al., 1978). Finally, values of oxygen metabolic rate were converted to molar units for stoichiometric comparisons with glucose utilization.

***Studies of glucose metabolism***

Studies of glucose metabolism were done using $^{18}$F-FDG (2-$^{18}$F-fluoro-2-deoxy-D-glucose) as a tracer. FDG distributes in tissue like glucose but remains unmetabolized in the form of 6-phosphate making quantitative imaging studies possible. The kinetic model of Sokoloff et al (Sokoloff et al., 1977) extended by Phelps (Phelps et al., 1979) was used in data analysis. Following a rapid intravenous injection of 5 mCi of $^{18}$F-FDG, dynamic PET images were acquired at a level 15 mm anterior from the earbar for 30 min. After this, coronal tomographic slices were acquired over the brain at 5 mm steps. Arterial blood samples were drawn for determination of plasma radioactivity. The data were fitted to a 2-exponential function and used as an input function in calculating glucose metabolic rate. In addition, arterial glucose values were determined before and after the experiment. Values for regional cerebral glucose metabolism were calculated using tissue data from the areas of interest and a value of 0.5 for the lumped constant (Reivich et al., 1985). Finally, the values of glucose metabolic rate were converted to molar units for stoichiometric comparison with $O_2$ consumption.

***Studies of dopamine D2 receptors and transporters***

Each study included two experiments. The first experiment was carried out with $^{11}$C-raclopride to investigate dopamine $D_2$ receptors, and the second experiment was conducted 2-3 hours later with $^{11}$C-CFT (2β-carbomethoxy-3 β -(4-fluorophenyltropane) in order to investigate dopamine transporters. Radiolabeled ligand, $^{11}$C-raclopride or $^{11}$C-CFT (6-8

mCi, specific activity 600-1000 mCi/μmol) was injected into the femoral vein; and imaging data were acquired stepwise on seven coronal brain levels, initially using 15 seconds per image. The acquisition time was subsequently increased to 60 seconds, the total imaging time being 90 minutes in both experiments. Eighteen arterial blood samples of 0.1 ml were drawn at different time points starting from 10 seconds frequency and ending with 15 minutes frequency in order to monitor the decrease in radioactivity. In addition, 3 arterial blood samples were drawn for HPLC analyses of metabolites of the labeled ligands.

Kinetic behavior of $^{11}$C-CFT was studied with a four-parameter estimation of the three compartmental model approach. In the three compartmental model, the first compartment is the plasma pool, the second is the exchangeable tracer pool including free and nonspecifically bound ligand in the brain, and the third compartment is a trapped tracer pool including bound ligand in the brain. The exchangeable tracer pool contains ligand but no receptors; and the third compartment includes all the receptors, partly or totally occupied by ligands. The kinetic parameters $k_3$ and $k_4$ describe the binding to and dissociation from the receptors.

The transfer coefficients $k_1$-$k_4$ were mathematically resolved using least square fit; Levenburg-Marquardt method. All numerical analyses were done with the optimization tool SAAM II (Foster et al., 1994). For stabilization of the k values the fitting procedure was performed using two steps. Since the cerebellum does not have specific receptor binding or is negligible, fitting was done with the cerebellar data, letting all the k-values float. The ratio $k_1/k_2$ was then calculated. In further iterations this fixed ratio was used as a constraint and applied with a sequential quadratic programming method combined with a cost function to reach parameter optimization. Regional binding potential was calculated as a ratio of $k_3/k_4$ (the ratio of the transport from the exchangeable tracer pool into the bound tracer pool to the transport from the bound tracer pool back into the exchangeable tracer pool). Regional binding potentials were calculated separately for left and right caudate, putamen, SN, thalamus, SMA and PMC.

## Results

### *Accuracy of the volumetric data analyses*

Development of image fusion and volumetric data analysis has been an essential part of this work. This approach is absolutely necessary to obtain reliable data from small brain regions. Figure 2 shows coronal, transverse and sagittal segmentation with 3 mm steps (slice thickness) of a volume rendered MR images fused with PET images of dopamine D2 receptor distribution after MPTP. The original PET images were acquired with 5 mm steps and a slice thickness of 5 mm. Figure 3 demonstrates selection of the regions of interest on a single slice level. The validation of the volumetric data analyses was done with a phantom of concentric spheres (Figure 4). Table II shows the accuracy of the obtained results based on the volumetric data analyses and actual measurement of radioactivity, with comparison to the conventional 2 dimensional pixel analyses.

**Table II. Radioactivity based on the volumetric data analyses compared to the measured radioactivity and the conventional 2-dimensional pixel analyses in two concentric spheres.**

| | **Inner sphere** | **Outer sphere** |
|---|---|---|
| Radioactivity based on the volumetric data analyses (μCi/100ml) | 527+/-20 | 239+/-7 |
| Measured radioactivity (μCi/100ml) | 516+/-5 | 225+/-4 |
| Conventional 2D ROI analyses (μCi/100ml) | 572+/-72 | 275+/-55 |

Both calculated radioactivity concentrations were higher than the real measured radioactivity because of the internal scatter. The absolute values calculated using volumetric data analyses were 2-6 % higher than measured radioactivity while conventional 2D pixel analyses gave 11-22% higher values.

These basic tools have been used to obtain data for the calculation of blood flow, oxygen extraction fraction and metabolism as well as glucose metabolism and binding parameters for dopamine transporters and dopamine D2 receptors in different brain regions.

***Hemodynamics and cerebral energy metabolism***

Figure 5 (see Table IV) shows the quantitative distribution of blood flow, oxygen metabolism, glucose metabolism, dopamine transporters, and dopamine D2 receptors at one midbrain level before and after MPTP. From these images it can be observed, that the most striking change after MPTP is the decrease in striatal dopamine transporter binding. Blood flow is enhanced in the basal ganglia, mainly because of enhanced physiological activity in the globus pallidus. Glucose metabolism, an indication of brain energy function, is decreased in all other brain regions but the GP, where an average of 15% increase is observed (see Table I). Figure 6 shows the quantitative topographic distribution of hemodynamic, metabolic and dopamine receptor function both before and after MPTP induced neurotoxicity that was obtained by volumetric data analyses. The largest decrease in blood flow after MPTP was observed in the primary motor cortex (39+/-4%). Blood flow was decreased in the striatal area (caudate and putamen) by 22-26%, in the thalamus by 17+/-3%, in the SN by 9+/-2% and in the SMA by only 4+/1%. In the globus pallidus, blood flow was increased by 15+/-3%. Oxygen extraction fraction was moderately enhanced in all brain areas after MPTP (Figure 6). Values for oxygen metabolism in the GP, SMA and SN were significantly elevated, partly being reflection of elevated oxygen extraction fraction. Oxygen metabolism was decreased in the putamen and caudate by 10+/2% and significantly in the PMC (23+/-2%). Glucose metabolism was decreased in all other brain areas but the GP (Figure 6). In the striatal area glucose utilization was decreased by 35+/17% in the caudate and 38+/-8% in the putamen, 25+/-7% in the thalamus and 6+/-2% in the SN. The highest decrease observed was in the PMC (50+/-12%), and the smallest in the SMA (1+/-1%). Glucose utilization was enhanced in the GP by 15+/-3% (see Table IV).

***Stoiciometry of glucose utilization and O2 consumption***

Table III shows the calculated values for stoichiometric balance in different brain areas before and after MPTP. The stoichiometric balance increased in all brain areas after MPTP, indicating that, in addition to glucose, other substrates were also metabolized after MPTP.

**Table III. Stoichiometry of glucose utilization and $O_2$ consumption in different brain areas before and after MPTP.**

| | Before MPTP | After MPTP |
|---|---|---|
| Putamen | 6.68+/-1.06 | 8.71+/-0.86 |
| Caudate | 5.13+/-0.69 | 6.92+/-0.34 |
| GP | 7.39+/-0.78 | 8.23+/-0.92 |
| Thalamus | 6.98+/-1.91 | 7.71+/-0.71 |
| SN | 5.28+/-0.41 | 7.86+/-0.43 |
| SMA | 5.63+/-0.89 | 5.84+/-0.32 |
| PMC | 4.19+/-0.53 | 6.00+/-0.54 |
| Cerebellum | 4.42+/-0.98 | 5.04+/-0.38 |

***Dopamine transporters and receptors***

The binding of $^{11}$C-CFT labeled dopamine transporters in presynaptic terminals is significantly decreased in the putamen (65+/-4%), caudate (62+/-5%), thalamus (39+/-4%), SN (36+/-3%), SMA (25+/-2%), and PMC (25+/-2%) (Figures 5 and 6). $^{11}$C-raclopride binding in dopamine D2 receptors shows overall decreases (Figures 5 and 6, Table IV). However, because of a large variation in the results there is no significant change in raclopride binding after MPTP.

***Studies of receptor function and metabolism in relation to neural circuitry***

To compare the obtained experimental results of dopamine receptor function, hemodynamics and metabolism with the known neural circuitry, we analyzed MPTP neurotoxicity induced changes in different brain areas, conventionally included in neurophysiological studies of the neural networks. Table IV shows the direction of MPTP induced significant changes in different brain areas.

**Table IV. MPTP induced changes in dopamine receptor function, hemodynamics and metabolism in different brain areas: ↑ indicates an increase, ↓ indicates a decrease and ↕ indicates no change compared to the pre MPTP value. * signs $p<0.05$ and ** $p<0.01$.**

| | Dopamine transporter | Dopamine D2 receptor | Blood flow | Oxygen extraction | Oxygen metab | Glucose metab |
|---|---|---|---|---|---|---|
| Putamen | ↓ ** | ↓ | ↓ ** | ↑ * | ↓ | ↓ ** |
| Caudate | ↓ ** | ↓ | ↓ ** | ↑ | ↓ | ↓ ** |
| GP | - | - | ↑ * | ↑ | ↑ ** | ↑ |
| Thalamus | ↓ ** | ↕ | ↓ * | ↕ | ↓ | ↓ |
| SN | ↓ ** | ↓ | ↓ | ↑ * | ↑ * | ↓ |
| SMA | ↓ * | ↓ | ↑ * | ↑ | ↑ * | ↕ |
| PMC | ↓ * | ↕ | ↓ ** | ↑ | ↓ ** | ↓ ** |
| Cerebellum | - | - | ↑ | ↑ | ↑ | ↓ |

**Discussion**

Parkinson's disease is characterized neuropathologically by a severe depletion of dopamine neurons in the basal ganglia. Our experiments, conducted in primates after MPTP induced neurotoxicity, showed significantly decreased binding of $^{11}$C-CFT in striatum, indicating depletion of presynaptic dopamine terminals. We have published this observation in 1992 (Hantraye et al., 1992), and in 1994 we further demonstrated the correlation to locomotor activity (Wullner et al., 1994). Since then, about 200 papers have been published, with a unanimous observation of declining dopamine transporter binding, (van Dyck et al., 2002;Antonini et al., 2001; Chouker et al., 2001; Huang et al., 2001; Marck et al., 2001; Sakakibara et al., 2001). Even though there is a unequivocal decline in presynaptic dopamine transporter binding in PD, there is inconsistency in reported results of $^{11}$C-raclopride binding in dopamine D2 receptors in PD (Doudet et al., 2000; Hwang et al., 2002; Kaasinen et al., 2000). In our present experiments, we have found a tendency for a decrease but with a large variation in dopamine D2 receptor binding after MPTP toxication. This outcome might be partly dependent on the criterion of selecting animals for this study. The dopamine transporter binding levels were decreased at least by 60% in addition to changed pattern of the locomotor activity

between day and night. We have earlier reported of a moderately increased $^{11}$C-raclopride binding in D2 receptors after an acute MPTP neurotoxicity, as well as after 6-hydroxydopamine toxicity (van Nguyen et al., 2000). Altogether, our observations of dopamine D2 receptor binding are consistent with a number of publications that propose a biphasic behavior of D2 receptor binding; indicating that in the early phase of Parkinson's disease, D2 receptor binding is enhanced because of supersensitivity and it will decline later with progression of the disease (Doudet et al., 2000; Hwang et al., 2002; Kaasinen et al., 2000). In addition to striatal receptor binding, we were able to investigate binding characteristics of $^{11}$C-CFT and $^{11}$C-raclopride in the thalamus, SN, SMA and PMC by using the volume of interest determined from the fusion with MR images. Using conventional PET image analysis it is impossible to localize these sites because the accumulation of radioactivity is so low compared to striatal accumulation. The binding values obtained (Figures 5 and 6) correlate well with the values obtained using autoradiographic techniques (Kaufman and Madras, 1992).

In addition to studies of dopamine transporters and dopamine D2 receptors, we conducted hemodynamic and metabolic studies in this preclinical model of PD with the ultimate aim of finding parallels to human PD in adaptive changes including metabolic neural networks and dopaminergic function.

Our observations after MPTP toxicity are consistent with changes seen in hemodynamic function and metabolism in PD (Brooks, 1997; Brooks, 1999; Eidelberg et al., 1995b; Schmidt and Ferger, 2001). Brooks et al have shown that slowness in free performed motion in PD patients corresponds with changes in blood flow in the supplementary motor area and dorsal prefrontal cortex; areas, which get subcortical input from the basal ganglia. Notably, blood flow changes consistent with a compensatory overactivation in lateral premotor area were observed. In PD, there appears to be a synchronization of GPe and GPi output signals as a result of the loss of DA tonic input to the putamen; that together with a reduced thalamic input to the SMA and PM cortices may explain the motor signs of PD (Brooks, 1999; Eidelberg et al., 1995b; Schmidt and Ferger, 2001). Moreover, the recruitment of more cortical regions and the increased and widespread activation of PM and SMA associated cortices suggest that these structures

are compensating for the abnormal input; to be able to activate the motor cortex for initiation of the movement (Brooks, 1997; Eidelberg et al., 1996).

We observed enhanced blood flow in the supplementary motor area as well as in the globus pallidus, while blood flow was decreased in the putamen, caudate and primary motor cortex of the parkinsonian primate. Oxygen metabolism was marginally enhanced in the globus pallidus and supplementary motor area and decreased in the putamen, caudate and primary motor cortex. Glucose metabolism was decreased in all brain areas after MPTP but the GP and SMA. In short, we found, 1) a decreased striatal dopamine transporter binding, indicating degeneration of presynaptic terminals; 2) an increased blood flow in the globus pallidus, indicating over activation in that brain area; 3) a decreased glucose metabolism in the thalamus, indicating decreased energy metabolism; and 4) decreased blood flow and glucose metabolism in the PMC, indicating decreased motor activity. However, at the same time, blood flow in the SMA was increased while no change in glucose metabolism was observed indicating a compensatory mechanism in motor function. These observations (see Table IV) support a neural circuitry based reasoning for changes seen in functional interactions of the motor system in human parkinsonism (DeLong and Wichman, 2001; Isacson et al., 2001).

In the normal *in vivo* state, glucose is the only substrate for energy metabolism in the brain. Under normal circumstances, no other potential energy yielding substrate has been found to be extracted from the blood in more than trivial amounts. For complete oxidation of glucose, the theoretical ratio of $O_2$ to glucose utilization is 6.0. In the present experiments, an average value for the stoichiometry of the glucose utilization and oxygen consumption is 5.8+/-0.6 before MPTP regimen and 7.0+/-0.9 after MPTP calculated as a mean of 8 investigated brain areas (see Table III). An average 20% increase in oxygen consumption compared to glucose utilization after MPTP may be explained by a reduced mitochondrial function. The obtained results of stoichiometric balance are also unique in the sense that they show that metabolic balance analysis (oxygen to glucose) is valid also during anesthesia.

To obtain quantitative information from small brain areas in imaging studies, we have developed a volumetric technique for data analyses and used fused PET and MRI data. In addition, the primate brain atlas was utilized to outline the regions of interest on

MR images. Even when the selection of the volume of interest is accurate on a technical level, there is a potential error in the absolute values because of effects of partial volume (Hoffman et al., 1979). Moreover, internal scatter radiation is a factor in nearby low activity tissue if the neighboring tissue has high activity concentration. In biological studies this shows up especially in the $^{11}$C-CFT studies of dopamine transporters, where the putamen has a high activity accumulation compared to the nearby tissues (Figures 5). To validate volumetric data analyses, imaging studies in concentric sphere phantoms were conducted. The absolute values calculated for radioactivity concentration were higher than measured radioactivity mainly because of the internal scatter. In the biological studies, converting count information into radioactivity values, the used calibration coefficient is obtained by similar volumetric data processing as the real data, and the effect of the internal scatter is therefore partially eliminated.

These experiments provide in-depth information on changes in metabolic and dopaminergic function in neural network after MPTP-induced parkinsonism in primates. This information is valuable for investigations of compensatory mechanism during degeneration and structural repair.

**Acknowledgements:** We wish to thank cyclotron operators William Bucklewicz and David Lee for preparing radiopharmaceuticals for these experiments as well as Jack McDowell for taking good care of the primates. This work was supported by DOD grant #DAMD17-98-1-8618 and NINDS grant #NS P50-39793 to O.I. at McLean Hospital and DOD grant #DAMD17-99-1-9555 to A-L.B. at Massachusetts General Hospital. FC was supported by the Medical Research Council of Canada.

## REFERENCES


Alexander G. Selective neuronal discharge in monkey putamen reflects intended direction of planned limb movement. Exp Brain Res 1987; 67: 623-634.

Alexander G, DeLong MR, Strick PL. Parallel organization of functionally segregated circuits linking basal ganglia and cortex. Ann Rev Neurosci 1986; 9: 357-381.

Alexander GE, Crutcher, MD, Delong, MR. Basal ganglia thalamo-cortical circuits: parallel substrates for motor, oculomotor, "prefrontal" and "limbic" functions. Prog Brain Res 1990; 85: 119-146.

Antonini A, Kazumata K, Feigin A, Mandel F, Dhawan V, Margouleff C, et al. Differential diagnosis of parkinsonism with [18F]fluorodeoxyglucose and PET. Mov Disord 1998; 13: 268-74.

Antonini A, Moresco RM, Gobbo C, De Notaris R, Panzacchi A, Barone P, et al. The status of dopamine nerve terminals in Parkinson's disease and essential tremor: a PET study with the tracer [11-C]FE-CIT. Neurol Sci 2001; 22: 47-8.

Antonini A, Vontobel P, Psylla M, Gunther I, Maguire PR, Missimer J, et al. Complementary positron emission tomographic studies of the striatal dopaminergic system in Parkinson's disease. Arch Neurol 1995; 52: 1183-90.

Berding G, Odin P, Brooks DJ, Nikkhah G, Matthies C, Peschel T, et al. Resting regional cerebral glucose metabolism in advanced Parkinson's disease studied in the off and on conditions with [18F]FDG-PET. Mov Disord 2001;16:1014-22.

Bohnen N, Minoshima S, Giordani B, Frey KA, Kuhl DE. Motor correlates of occipital glucose hypometabolism in Parkinson's disease without dementia. Neurology 1999; 52: 541-546.

Brooks D. PET and SPECT studies in Parkinson's disease. Baillieres Clin Neurol 1997; 6: 69-87.

Brooks D. Functional imaging of Parkinson's disease: is it possible to detect brain areas for specific symptoms? J Neural Transm Suppl 1999; 56: 139-53.

Brooks DJ. Cerebral blood flow activation studies. In: Calne D, Calne S, editors. Parkinson's Disease: Advances in Neurology. Vol 86. Philadelphia: Lippincott Williams & Wilkins; 2001. p. 225-235.

Brownell A-L, Jenkins BG, Elmaleh DR, Deacon TW, Spealman RD, Isacson O. Combined PET/MRS brain studies show dynamic and long-term physiological changes in a primate model of Parkinson disease. Nature Medicine 1998; 4: 1308-1312.

Brownell A-L, Jenkins BG, Isacson O. Dopamine imaging markers and predictive mathematical models for progressive degeneration in Parkinson's disease. Biomedicine and Pharmacotherapy 1999; 53: 131-40.

Brownell GL, Burnham CA, Stearns CW, Chesler DA, Brownell A-L, Palmer M. Development in high-resolution positron emission tomography at MGH. Int J Img Systems and Technol 1989; 1: 207-17.

Checkoway H, Nelson LM. Epidemiologic approaches to the study of Parkinson's disease etiology. Epidemiology 1999; 10: 327-36.

Chouker M, Tatsch K, Linke R, Pogarell O, Hahn K, Schwarz J. Striatal dopamine transporter binding in early to moderately advanced Parkinson's disease: monitoring of disease progression over 2 years. Nucl Med Commun 2001; 22: 721-5.

Crutcher M, DeLong MR. Single cell studies of the primate putamen. II. Relations to direction of movement and pattern of muscular activity. Exp Brain Res 1984; 53: 244-258.

DeLong M, Wichman T. Deep brain stimulation for Parkinson's disease. Ann Neurol 2001; 49: 142-143.

Doudet DJ, Holden JE, Jivan S, McGeer E, Wyatt RJ. In vivo PET studies of the dopamine D2 receptors in rhesus monkeys with long term MPTP-induced parkinsonism. Synapse 2000; 38: 105-13.

Eberling J, Richardson BC, Reed BR, Wolfe N, Jagust WJ. Cortical glucose metabolism in Parkinson's disease without dementia. Neurobiol Aging 1994; 15: 329-335.

Eidelberg D, Moeller JR, Ishikawa T, Dhawan V, Spetsieres P, Chaly T, et al. Assessment of disease severity in Parkinsonism with fluorine-18-fluorodeoxyglucose and PET. J Nucl Med 1995a; 36: 378-383.

Eidelberg D, Moeller JR, Ishikawa T, Dhawan V, Spetsieres P, Chaly T, et al. Early differential diagnosis of Parkinson's disease with 18F-fluorodeoxyglucose and positron emission tomography. Neurology 1995b; 45: 1995-2004.

Eidelberg D, Moeller JR, Ishikawa T, Dhawan V, Spetsieres P, Silbersweig D, et al. Regional metabolic correlates of surgical outcome following unilateral pallidotomy for Parkinson's disease. Ann Neurol 1996; 39: 452-9.

Foster D, Barrett PHR, Bell BM, Beltz WF, Cibelli C, Golde H, et al. Simulation, analysis and modeling software. BMES Bull 1994; 18.

Frackowiak R, Lenzi GL, Jones T, Heather JD. Quantitative measurement of regional cerebral blood flow and oxygen metabolism in man using 15O and positron emission tomography: Theory, procedure and normal values. J Comput Assist Tomogr 1980; 4: 727-736.

Fukuda M, Mentis MJ, Ma Y, Dhawan V, Antonini A, Lang AE, et al. Networks mediating the clinical effects of pallidal brain stimulation for Parkinson's disease. A PET study of resting-state glucose metabolism. Brain 2001; 124: 1601-1609.

Gorrell J, DiMonte D, Graham D. The role of environment in Parkinson's disease. Environmental Health Perspective 1996; 104: 652-4.

Hantraye P, Brownell A-L, Elmaleh DR, Spealman RD, Wullner U, Brownell GL, et al. Dopamine fiber detection by [11C]-CFT and PET in a primate model of parkinsonism. Neuroreport 1992; 3: 265-8.

Hoffman EJ, Huang SC, Phelps ME. Quantitation in positron emission tomography. 1 - Effect of object size. J Comp Assist Tomogr 1979; 3: 299-308.

Huang HS, Lin CZ, Lin JC, Wey SP, Ting G, Liu RS. Evaluation of early-stage Parkinson's disease with 99mTc-TRODAT-1 imaging. J Nucl Med 2001; 42: 1303-8.

Hwang WJ, Yao WJ, Wey SP, Shen LH, Ting G. Downregulation of striatal dopamine D2 receptors in advanced Parkinson's disease contributes to the development of motor flunctuation. Eur Neurol 2002; 47: 113-117.

Imon Y, Matsuda H, Ogawa M, Kogure D, Sunohara N. SPECT image analysis using statistical parametric mapping in patients with Parkinson's disease. J Nucl Med 1999; 40: 1583-9.

Isacson O, van Horne C, Schumacher JM, Brownell A-L. Improved surgical cell therapy in Parkinson's disease - Physiological basis and new transplantation methodology. In: Calne D, Calne S, editors. Parkinson's Disease: Advances in Neurology. Vol 86. Philadelphia: Lippincott Williams & Wilkins; 2001. p. 447-454.

Jones T, Chesler DA, Ter-Pogossian MM. The continuous inhalation ofxygen-15 for assessing regional oxygen extraction fraction in the brain of man. Br J Radiol 1976; 49: 339-343.

Kaasinen V, Ruottinen HM, Nagren K, Lehikoinen P, Oikonen V, Rinne JO. Upregulation of putaminal D2 receptors in early Parkinson's disease: a comparative PET study with [11C]raclopride and [11C]N-methylspiperoni. J Nucl Med 2000; 41: 65-70.

Kaufman MJ, Madras BK. Distribution of cocaine recognition sites in monkey brain: II.Ex vivo autoradiography with [3H]CFT and [125I]RTI-55. Synapse 1992; 12: 99-111.

Kish S, Shannak K, Hornykiewicz O. Uneven pattern of dopamine loss in the striatum of patients with idiopathic Parkinson's disease. N Engl J Med 1988; 318: 876-880.

Marck K, Innis R, van Dyck C, Fussel B, Early M, Eberly S, et al. [123I]beta-CIT SPECT imaging assessment of the rate of Parkinson's disease progression. Neurology 2001; 57: 2089-94.

Markus H, Lees AJ, Lennox G, Marsden CD, Costa DC. Patterns of regional cerebral blood flow in corticobasal degeneration studied using HMPAO SPECT; comparison with Parkinson's disease and normal controls. Mov Disord 1995; 10: 179-187.

Marsden CD. Parkinson disease. Postgrad Med J 1992; 68: 538-43.

Mizuno Y, Shimoda-Matsubayashi S, Matsumine H, Morikawa N, Hattori N, Kondo T. Genetic and environmental factors in the pathogenesis of Parkinson's disease. Adv Neurol 1999; 80: 171-9.

Moeller JR, Eidelberg D. Divergent expression of regional metabolic topographies in Parkinson's disease and normal aging. Brain 1997; 120: 2197-206.

Palombo E, Porrino LJ, Bankiewicz KS, Crane AM, Sokoloff L, Kopin IJ. Local cerebral glucose utilization in monkeys with hemiparkinsonism induced by intracarotid infusion of the neurotoxin MPTP. J Neurosci 1990; 10: 860-869.

Palombo E, Porrino LJ, Crane AM, Bankiewicz KS, Kopin IJ, Sokoloff L. Cerebral metabolic effects of monoamine oxidase in normal and 1-methyl-4-phenyl-1,2,3,6-tetrahydropyridine acutely treated monkeys. J Neurochem 1991; 56: 1639-46.

Phelps ME, Huang SC, Hoffman EJ, Selin C, Sokoloff L, Kuhl D. Tomographic measurement of local cerebral glucose metabolic rate in humans with (F-18-2-fluoro-2-deoxy-D-glucose: Validation of method. Ann Neurol1979; 6: 371-88.

Porrino L, Burns RS, Crane AM, Palombo E, Kopin IJ, Sokoloff L. Changes in local cerebral glucose utilization associated with Parkinson's syndrome induced by 1-methyl-4-phenyl-1,2,3,6-tetrahydropyridine (MPTP) in the primate. Life Sci 1987; 40: 17657-64.

Puyau M, Adolph AL, Vohra FA, Butte NF. Validation and calibration of physical activity monitors in children. Obes Res 2002; 10: 150-7.

Reivich M, Alavi A., Wolf A., Fowler J, Russell J, Arnett C, et al. Glucose metabolism rate kinetic model parameter determination in humans: The lumped constants and rate constants for [18F]fluorodeoxy- and [11C]deoxyglucose. J Cereb Blood Flow Metab 1985; 5: 179-192.

Sakakibara R, Shinotoh H, Yoshiyama M, Hattori T, Yamanishi T. SPECT imaging of the dopamine transporter with [123I]-beta-CITreveals marked decline of nigrostriatal dopaminergic function in Parkinson's disease with urinary dysfunction. J Neurol Sci 2001; 187: 55-9.

Samuel M, Ceballos-Baumann AO, Turjanski N, Boecker H, Gorospe A, Linazasoro G, et al. Pallidotomy in Parkinson's disease increases supplementary motor area and prefrontal activation during performance of volitional movements: an H2(15)O PET study. Brain 1997; 120: 1301-13.

Schapira AHV. Neurotoxicity and the mechanisms of cell death in Parkinson's disease. In: Battistin L, Scarlato G, Carceni T and Ruggieri S, editors. Advances in Neurology. Vol 69. Philadelphia: Lippincott-Raven, 1996: 161-165.

Schmidt N, Ferger B. Neurochemical findings in the MPTP model of Parkinson's disease. J Neural Transm 2001; 108: 1263-82.

Sokoloff L, Reivich M, Kennedy C, Des Rosiers MH, Patlak CS, Pettigrew KD, et al. The (C-14) deoxy glucose method for the measurement of local cerebral glucose utilization: Theory, procedure, the normal values in the conscious and anesthetized albino rat. Neurochem 1977; 28: 897-916.

Subramanyam R, Alpert NM, Hoop B Jr, Brownell GL, Taveras JM. A model for regional cerebral oxygen distribution during continuous inhalation of 15O2, C15O, and C15O2. J Nucl Med 1978; 19: 43-53.

van Dyck C, Seibyl JP, Malison RT, Laruelle M., Zoghbi SS., Baldwin RM, et al. Age-related decline in dopamine transporters: analysis of striatal subregions, nonlinear effects, and hemispeheric asymmetries. Am J Geriatr Psychiatry 2002; 10: 36-43.

van Nguyen T, Brownell A-L, Chen YI., Livni E., Coyle JT, Rosen BR, et al. Detection of the effects of dopamine receptor supersensitivity using pharmacological MRI and correlation with PET. Synapse 2000; 36: 57-65.

Wichman T, DeLong MR. Functional and pathophysiological models of the basal ganglia. [Review]. Curr Opin Neurobiol 1996; 6: 751-8.

Wullner U, Pakzaban P, Brownell A-L, Hantraye P, Burns L, Shoup T, et al. Dopamine terminal loss and onset of motor symptoms in MPTP-treated monkeys: A positron emission tomography study with 11C-CFT. Exp Neurol 1994; 126: 305-9.

## FIGURE LEGENDS

Figure 1. Effect of MPTP induced neurotoxicity on spontaneous locomotor activity detected by an Actiwatch before and after MPTP. Before MPTP there was a significant difference between day and night time locomotor activity, while after MPTP no activity difference was observable.

Figure 2. A PET study of the distribution of $^{11}$C-raclopride binding in dopamine D2 receptors after MPTP toxicity in a primate brain. PET data were fused with volume rendered MR images. The upper row shows coronal slices from anterior to posterior direction. Binding to D2 receptors are localized mainly in the putamen and caudate. The middle row shows sagital slices from right to left. The slices 1-7 represent right hemisphere and the slices 8-13 left hemisphere. At the bottom row transverse slices are shown from top to base. Volumetric distribution of radioactivity is used in selecting region (volumes) for interest used in quantitative data analyses of receptor function.

Figure 3. Anatomical borderlines observed from MR images were used to define the regions of interest for volumetric data analysis on the fused PET-MRI data set. Segmented brain areas are numbered and color coded as shown in the image. The data from the left and right hemispheres were analyzed separately.

Figure 4. To evaluate the accuracy of the volumetric data reconstruction a phantom consisting of two concentric spheres was imaged by PET. Coronal PET images were acquired with 5 mm steps and slice thickness of 5 mm over the phantom. The middle row shows images, when the outer sphere was filled with $^{18}$F-labeled water and the inner sphere with water without radioactivity. The lower row shows images, when the inner sphere was filled with the same radioactivity concentration as above and activity concentration in the outer shell was about 44% of it. For data analysis PET images were fused with T2 weighted MR images and radioactivity concentration in the inner and outer

shell was determined (Table II) using the same volumetric data analysis as in the experimental primate studies.

Figure 5. Coronal midbrain slices of a monkey brain illustrate the quantitative distribution of hemodynamic, metabolic and dopamine receptor function before and after MPTP neurotoxicity: Studies of blood flow were conducted with a steady state inhalation technique using $C^{15}O_2$ gas mixture (Jones, 1976); Studies of oxygen metabolism were conducted with a steady state inhalation technique using $^{15}O_2$ gas mixture (Jones, 1976; Subramanyam, 1978); Studies of glucose metabolism were conducted with $^{18}$F-FDG (2-$^{18}$F-fluoro-2-deoxy-D-glucose); Studies of dopamine transporters were conducted with $^{11}$C-CFT (2B-carbomethoxy-3B-(4-fluorophenyltropane); Studies of dopamine D2 receptors were conducted with 11C-raclopride.

Figure 6. Quantitative topographic distribution (Mean +/-SEM) of hemodynamic, metabolic and dopamine receptor function before and after MPTP induced neurotoxicity in the different brain areas. All the data analyses are based on volumetric data analyses using fused PET and MR images. Significant difference was calculated as compared to the pre-MPTP values by using Dunnett's t test. Blood flow studies show significant decrease in putamen, caudate and PMC ($p<0.01$) and thalamus ($p<0.05$)and increase in GP and SMA ($p<0.05$) Oxygen extraction fraction (OER) shows overall increase with significant changes in putamen and SN ($p<0.05$). Oxygen metabolism shows significant increase in the GP ($p<0.01$), SN and SMA ($p<0.05$) and significant decrease in PMC ($p<0.01$) and overall decrease in the other brain areas. Glucose metabolism shows significant decrease in putamen, caudate and PMC ($p<0.01$) and overall decrease in the other brain areas but GP and SMA. Dopamine transporter binding investigated by $^{11}$C-CFT shows significant decrease in putamen, caudate, thalamus and SN ($p<0.01$) and SMA and PMC ($p<0.05$). Dopamine D2 receptor binding investigated by $^{11}$C-raclopride does not show any significant changes.

Figure 1.

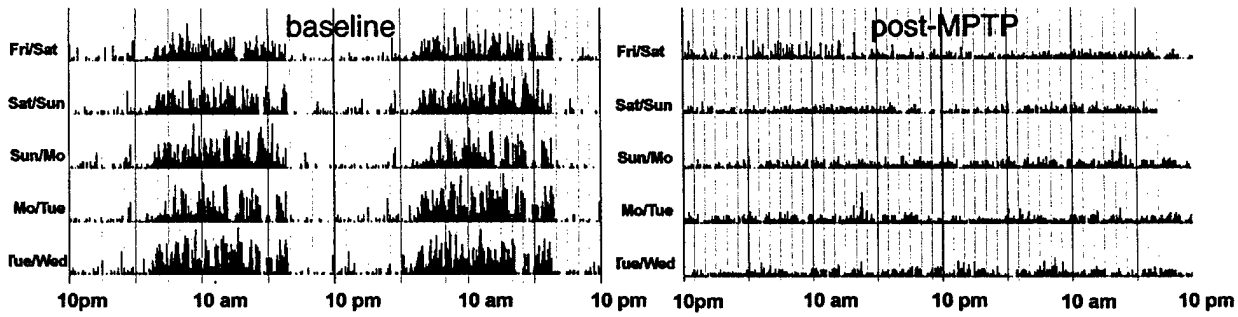
baseline
post-MPTP
Fri/Sat
Sat/Sun
Sun/Mo
Mo/Tue
Tue/Wed
10pm
10 am
10 pm
10 am
10 pm
10pm
10 am
10 pm
10 am
10 pm

Figure 2.

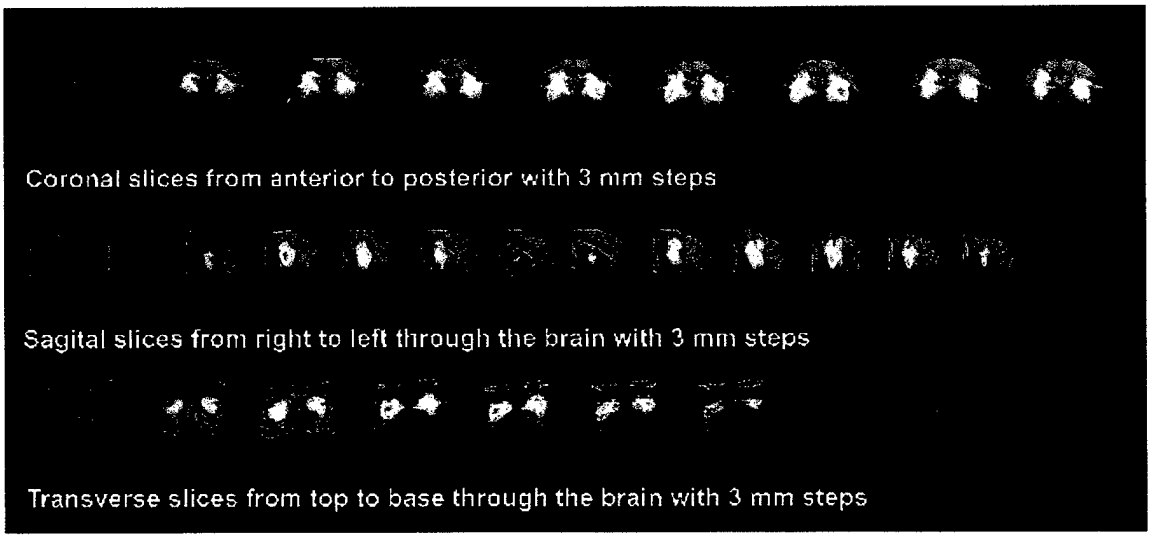
Coronal slices from anterior to posterior with 3 mm steps
Sagital slices from right to left through the brain with 3 mm steps
Transverse slices from top to base through the brain with 3 mm steps

Figure 3.

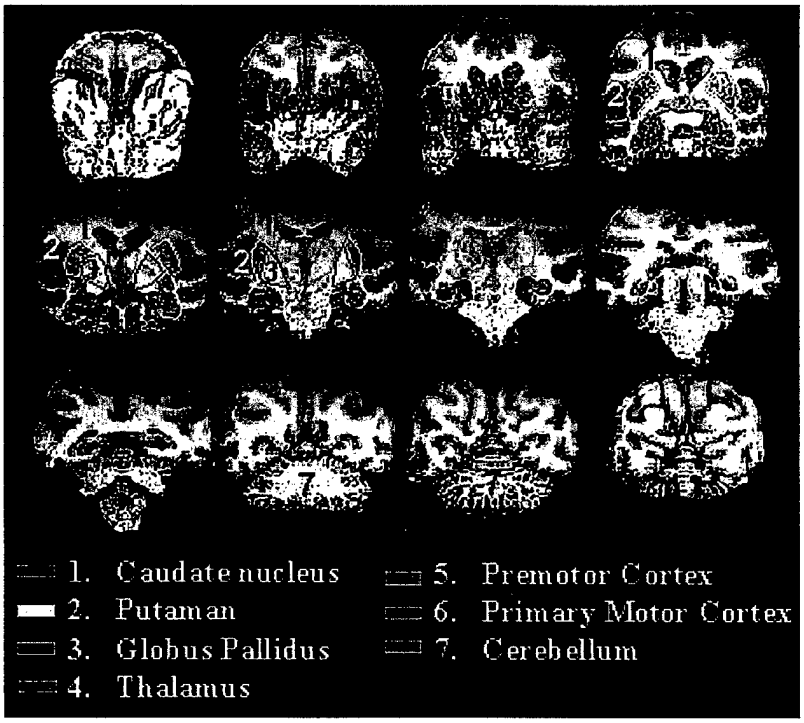
1. Caudate nucleus
2. Putaman
3. Globus Pallidus
4. Thalamus
5. Premotor Cortex
6. Primary Motor Cortex
7. Cerebellum

Figure 4.

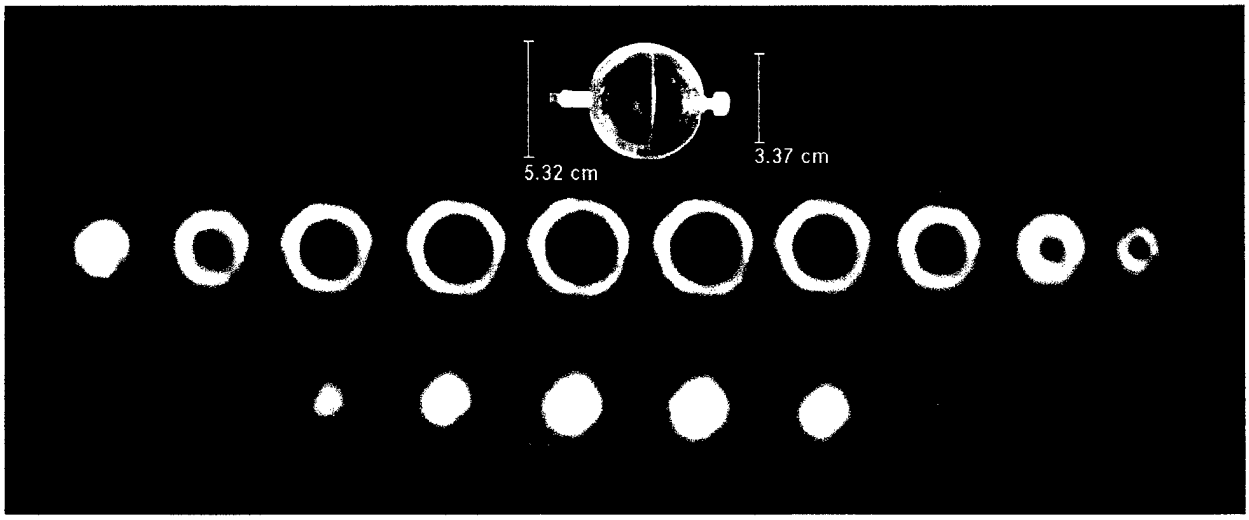

Figure 5.

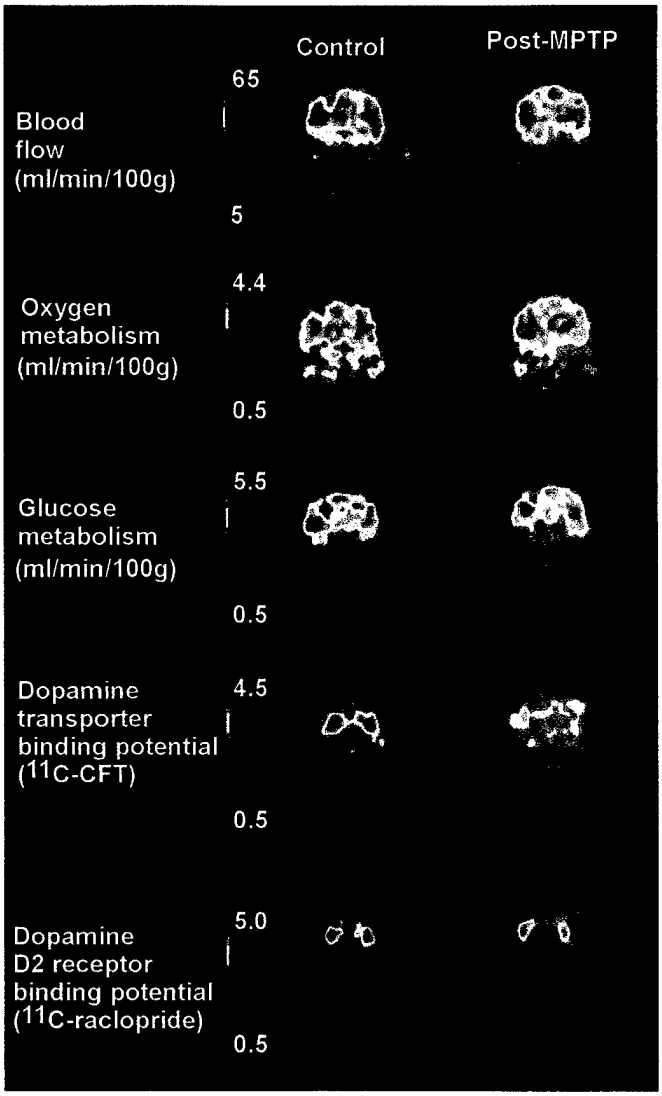
Control
Post-MPTP
Blood flow (ml/min/100g)
65
5
Oxygen metabolism (ml/min/100g)
4.4
0.5
Glucose metabolism (ml/min/100g)
5.5
0.5
Dopamine transporter binding potential ($^{11}$C-CFT)
4.5
0.5
Dopamine D2 receptor binding potential ($^{11}$C-raclopride)
5.0
0.5

Figure 6.

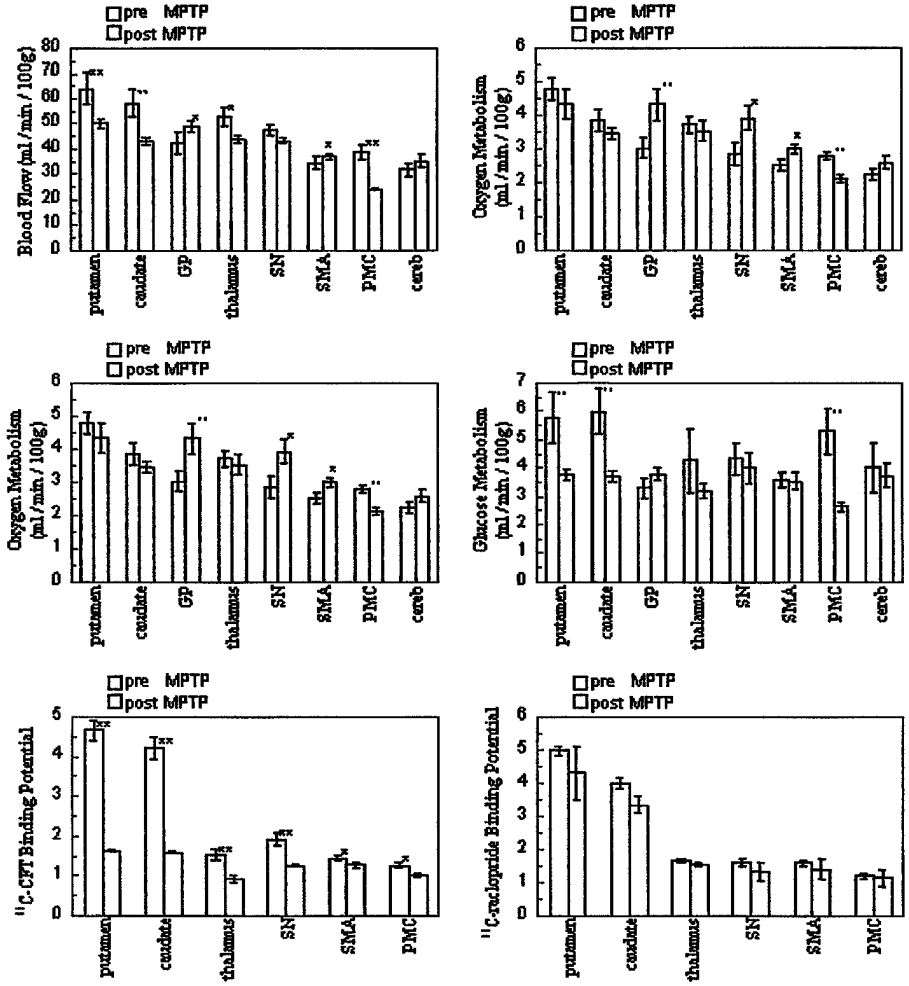
pre MPTP
post MPTP
Blood Flow (ml / min / 100g)
Oxygen Metabolism (ml / min / 100g)
Glucose Metabolism (ml / min / 100g)
$^{11}$C-CFT Binding Potential
$^{11}$C-raclopride Binding Potential
putamen
caudate
GP
thalamus
SN
SMA
PMC
cereb